

AUTOMATED DETECTION OF SUBMERGED NAVIGATIONAL
OBSTRUCTIONS IN FRESHWATER IMPOUNDMENTS WITH
HULL MOUNTED SIDESCAN SONAR

Approved by:

Dr. Mitchel A. Thornton, Advisor

Dr. Theodore Manikas

Dr. Sukumaran Nair

AUTOMATED DETECTION OF SUBMERGED NAVIGATIONAL
OBSTRUCTIONS IN FRESHWATER IMPOUNDMENTS WITH
HULL MOUNTED SIDESCAN SONAR

A Thesis Presented to the Graduate Faculty of
Bobby B. Lyle School of Engineering
Southern Methodist University

in

Partial Fulfillment of the Requirements

for the degree of

Master of Science in Computer Engineering

with a

Major in Computer Engineering

by

Phillip A. Morris

(B.S.Cp.E. University of South Florida)
(B.S.C.S. University of South Florida)

August 5, 2015

Morris, Phillip A.

B.S.Cp.E., University of South Florida, 2001
B.S.C.S., University of South Florida, 2001

Automated Detection of Submerged Navigational
Obstructions in Freshwater Impoundments With
Hull Mounted Sidescan Sonar

Advisor: Professor Mitchell A. Thornton

Master of Science conferred August 5, 2015

Thesis completed July 10, 2015

The prevalence of low-cost side scanning sonar systems mounted on small recreational vessels has created improved opportunities to identify and map submerged navigational hazards in freshwater impoundments. However, these economical sensors also present unique challenges for automated techniques. This research explores related literature in automated sonar imagery processing and mapping technology, proposes and implements a framework derived from these sources, and evaluates the approach with video collected from a recreational grade sonar system. Image analysis techniques including optical character recognition and an unsupervised computer automated detection (CAD) algorithm are employed to extract the transducer GPS coordinates and slant range distance of objects protruding from the lake bottom. The retrieved information is formatted for inclusion into a spatial mapping model.

Specific attributes of the sonar sensors are modeled such that probability profiles may be projected onto a three dimensional gridded map. These profiles are computed from multiple points of view as sonar traces crisscross or come near each other. As lake

levels fluctuate over time so do the elevation points of view. With each sonar record, the probability of a hazard existing at certain elevations at the respective grid points is updated with Bayesian mechanics. As reinforcing data is collected, the confidence of the map improves. Given a lake's current elevation and a vessel draft, a final generated map can identify areas of the lake that have a high probability of containing hazards that threaten navigation.

The approach is implemented in C/C++ utilizing OpenCV, Tesseract OCR, and QGIS open source software and evaluated in a designated test area at Lake Lavon, Collin County, Texas.

TABLE OF CONTENTS

LIST OF TABLES	viii
LIST OF FIGURES	ix
GLOSSARY	xii
ACKNOWLEDGEMENTS	xiii
Chapter	
1. INTRODUCTION	1
2. BACKGROUND	6
2.1 Side Scanning Sonar	6
2.2 Side Scanning Sonar Interpretation	7
2.3 Recreational Side Scanning Sonars	9
2.4 Automated Interpretation of Side Scan Sonar Imagery	11
2.5 Occupancy Grids	12
2.6 Transforming Coordinate Systems	16
2.7 WGS-84 Datum	21
3 RELATED WORKS	22
3.1 “A Bayesian approach to object detection in sidescan sonar”	22
3.2 “A Novel Technique for Mapping Habitat in Navigable Streams Using Low-cost Side Scan Sonar”	22

3.3 “Map uncertainties for unmanned underwater vehicle navigation using sidescan sonar”	23
4 MODELING AND DESIGN	24
4.1 Overview	24
4.2 Collection of Sonar Traces	24
4.3 Image Analysis of the Sonar Traces	25
4.3.1 Screen Division	26
4.3.2 Optical Character Recognition	27
4.3.3 Sonar Channel Image Processing and CAD	27
4.3.3.1 Histogram Statistics Generation	27
4.3.3.2 CAD	28
4.3.4 File Output	29
4.4 Spatial and Temporal Analysis	29
4.4.1 File Input	31
4.4.2 Projection Transform Class	31
4.4.3 Sonar Spatial Interpretation Model	32
4.4.4 Localization Uncertainty Model	34
4.4.5 Gridded Map Update	34
4.4.6 Elevation Specific Hazard Map	34
4.5 Generation of Maps	35

5	SONAR COLLECTION METHODOLOGY	36
5.1	Sonar Imagery Collection Parameters	36
5.2	Designated Study Area	37
5.3	Trip Summary	42
5.3.1	Data Collection April 4, 2015	43
5.3.2	Data Collection April 15, 2015	43
5.3.3	Data Collection May 1, 2015	44
6	RESULTS	45
6.1	Sonar Video Capture and Optical Character Recognition	45
6.1.1	Scan Converted Video	45
6.1.2	HumViewer Converted Video	45
6.1.3	General Observations	46
6.2	Pixel Brightness Normalization	48
6.3	CAD Results	49
6.4	Bathymetry	53
6.5	LCC Projection Class	54
6.6	Slant Range Distance of Identified Hazards	54
6.7	Elevation Hazard Maps	57
6.8	New Hazards at Higher Lake Elevations	60

7	CONCLUSION	62
	7.1 Conclusion	62
	7.2 Benchmarking	
	7.3 Improved CAD Technologies	63
	7.4 Improved Sensor Fusion	64
	7.4 Fusion with Additional Sensors	65
	7.5 Automated Collection	65
	APPENDIX	
	A. HARDWARE AND SOFTWARE	66
	B. USEFUL SCRIPTS	67
	C. PIXEL BRIGHTNESS DISTRIBUTIONS	68
	D. CATALOG OF SONAR VIDEOS CREATED	69
	E. PERMISSION TO USE PHOTOGRAPHY	72
	F. DUAL CHANNEL DETECTION CRITERIA	74
	REFERENCES	76

LIST OF TABLES

Table 2.5.1 - Bayes' Theorem Parameters	14
Table 2.5.2 – Occupancy Update Model	15
Table 2.5.3 – Additional Works in Gridded Occupancy Mapping	16
Table 2.6.1 - LCC Transform Equations Parameters	17
Table 2.6.2 - LCC Transform Constants	18
Table 2.6.3 - Forward Projection Algebraic Equations	19
Table 2.6.4 - Inverse Projection Algebraic Equations	19
Table 2.7 - WGS-84 Datum	21
Table 5.2 – LCC Projection Parameters for Study Area	37
Table 5.3 – Study Area Lake Levels	42
Table 6.6 – Hazard Identification Key	54
Table A.1 – Hardware Tools	67
Table A.2 – Software Tools	67
Table D.1 – 800 KHz Sonar Video Recorded April 4, 2015	70
Table D.2 – 800 KHz Sonar Video Recorded April 15, 2015	70
Table D.3 – 800 KHz Sonar Video Recorded May 1, 2015	70
Table D.4 – 455 KHz Sonar Video Recorded May 1, 2015	71

LIST OF FIGURES

Figure 1 - Sloop “Orion” After Striking a Submerged Tree in Lake Ray Hubbard, Texas	2
Figure 2.1.1 - Sonar Distance Terminology	6
Figure 2.1.2 - Equivalent Slant Range	7
Figure 2.2 – Example Side Scan Imagery	8
Figure 2.5 – Sensor Integration Framework	14
Figure 2.6 – Projection Transforms	17
Figure 4.4 – Sensor Integration Approach	30
Figure 4.4.2 – LCC Class UML	32
Figure 4.4.3.1 – 800 KHz Sonar Sensor Model	33
Figure 4.4.3.2 – 455 KHz Sonar Sensor Model	33
Figure 4.4.3.3 – Collision Sensor Model	34
Figure 4.5 – QGIS Project Screenshot	35
Figure 5.1 – Sonar Installation Parameters	36
Figure 5.2.1 – Designated Study Area	38
Figure 5.2.2 – Designated Study Area on October 18, 2013	39
Figure 5.2.3 – Identified Hazards in Designated Study Area North	40
Figure 5.2.4 – Identified Hazards in Designated Study Area Central	40
Figure 5.2.3 – Identified Hazards in Designated Study Area South	41

Figure 5.2.3 – Identified Hazards in Designated Study Area West	41
Figure 5.3.1 – 800 KHz Sonar Collection Route April 4	43
Figure 5.3.2 – 800 KHz Sonar Collection Route April 15	43
Figure 5.3.3 – 800 KHz Sonar Collection Route May 1	44
Figure 5.3.4 – 455 KHz Sonar Collection Route May 1	44
Figure 6.1.3 – Sonar Movie Created With HumViewer	47
Figure 6.2 - Pixel Brightness Histogram Statistics	49
Figure 6.3.1 – CAD Results Too Far	50
Figure 6.3.2 – CAD Correct Example 1	50
Figure 6.3.3 – CAD Correct Example 2	51
Figure 6.3.4 – CAD False Detection	51
Figure 6.3.5 – CAD Correct Example 3	52
Figure 6.3.5 – CAD Misses Part of a Submerged Tree	52
Figure 6.4 – Summary of Bathymetry Data	53
Figure 6.6.1 - Hazards Identified April 4, 2015	55
Figure 6.6.2 - Hazards Identified April 15, 2015	56
Figure 6.6.3 - Hazards Identified May 1, 2015	56
Figure 6.7.1 - Hazard Map Lake Elevation of 486 Feet	58
Figure 6.7.2 - Hazard Map Lake Elevation of 489 Feet	59
Figure 6.7.3 - Hazard Map Lake Elevation of 493 Feet	60

Figure 6.8 – Additional Hazards	61
Figure C - Pixel Brightness Histogram Statistics	69
Figure F.1 – Dual Channel Hazards Identified April 4, 2015	74
Figure F.2 – Dual Channel Hazards Identified April 15, 2015	75
Figure F.3 – Dual Hazards Identified May 1, 2015	75

GLOSSARY

Easting	Eastward measured distance along a Cartesian projected plane.
Ensonify	To fill a medium with sound for measurement and analysis for an acoustic sensor.
Northing	Northward measured distance along a Cartesian projected plane.
Outboard Motor	Propulsion system commonly found on small watercraft. It can pivot vertically and horizontally on a mounting bracket attached directly to the vessel's transom.
Port	Nautical term that refers to the left side of the vessel as perceived by an occupant when facing the bow.
Reverberation	Sound reflected from the surface of an object.
Starboard	Nautical term that refers to the right side of the vessel as perceived by an occupant when facing the bow.
Towfish	A platform towed behind a vessel with a cable or rope to house a side scanning sonar.
Transducer	A device that emits acoustic bursts of energy for measurement.
Transom	Nautical term that refers to the extreme aft or stern portion of a vessel's hull.

ACKNOWLEDGEMENTS

During my pursuit of graduate education, I've received help from a number of people that I would like to acknowledge. First I would like to thank my advisor, Dr. Mitch Thornton for his direction during my graduate studies at SMU, and his support in pursuing a research topic that does not strictly align with my coursework. I would also like to thank my thesis committee members, Dr. Theodore Manikas and Dr. Sukumaran Nair. I owe an endless debt of gratitude to my parents, Dr. and Mrs. Raymond Morris for their encouragement and support of my education. For my thesis research, they also gave me the direction to investigate papers related to spatial statistics.

As a Camber Corporation employee, I'm fortunate to have an employer that supports advanced education. I would like to thank my supervisor Lawson Reilly for giving me flexibility in my work schedule to make trips to campus during business hours as well as get my boat out on the lake to conduct research. My coworker Jay Williams was a great asset in helping me understand map projection concepts. Kathy Doyle with human resources played a vital role by providing proctoring. I would also like to thank Debra McDowell and Beth Minton at the SMU CSE department for all of their help in coordinating my distance coursework.

Most importantly I would like to thank my wife, Christina. Graduate school would simply not be a possibility without her support.

Chapter 1

INTRODUCTION

Submerged navigational hazards have long plagued boaters on freshwater impoundments. During periods of drought lake levels drop and a countless number of submerged timber and other structures begin to approach the surface. When rain begins to fill the lakes, exposed hazards become invisible as they slip just below the water's surface. As the lake levels fluctuate so do the locations and numbers of boating hazards. This can negate the knowledge of experienced boaters who often come to think of certain lake areas as being safe and hazard free, but are unfamiliar with the obstructions at the water's current elevation [1, 5, 6, 51].

"There's a lot of underwater hazards that are new, coming up daily, weekly," - B.J. Parkey, U.S. Army Corps of Engineers, speaking about conditions at Lake Texoma on January 2014 [4].

Striking these submerged hazards can be costly and extremely dangerous for boaters. Watercraft may become impaled, capsized, swamped, and/or possibly sink as shown in Figure 1. There have been documented cases of outboard motors striking submerged objects and flipping into the boat potentially crushing occupants and striking them with a rapidly spinning propeller [2]. If the collision occurs at high speed, the occupants may also be ejected from the boat. Rescue and salvage operations may be hampered by the same hazards. [1, 3, 4, 6]



Figure 1 - Sloop “Orion” After Striking a Submerged Tree in Lake Ray Hubbard, Texas [6, 7]

Photograph courtesy of Planet Rockwall.com

Despite the combined efforts of various government authorities, only a fraction of these obstacles has been identified or removed. Government agencies typically only have the resources to focus on hazards inside popular navigation channels often referred to as boat lanes. When water levels fall below historical averages, even these popular channels become inadequately marked [3, 8].

“The LCRA is trying to mark hazards in the lake with orange buoys, but it's impossible to mark all these obstructions,” – Don Brent, Lower Colorado River Authority (LCRA), Chief of Public Safety, speaking about conditions in Lake Travis on June 2011 [8].

There are a number of commercial maps and products available; however, none of them addresses the volume of hazards presented by variable lake levels. Commercially printed maps are available for most lakes and provide course bathymetry data. Areas of

the lake containing large amounts of timber are sometimes denoted by black dots; however, timber height is not available. The dots do not represent a comprehensive mapping of standing timber. Several other types of hazards such as large rocks, pilings, and other structures may also be noted on the maps, but again only represent a small subset of what actually exists in the lake. Also, the hazards indicated tend to be most representative of the lake when it is at a historical normal or full pool level as opposed to a drought or flood condition.

Digital maps are also available from various vendors. They may be viewed on navigational display systems and as applications that run on cell phones, tablets, and other handheld mobile devices. Compared to their printed counterparts, digital maps usually provide finer bathymetry data as well embedded notes on areas of interest such as possible fishing locations and some navigational hazards. Some of the latest maps also have an interface for conforming bathymetry data to a lake level adjustment control. Digital maps have also introduced a form of social media that allows boaters to share notes and points of interest with each other over an internet connection [12].

Other products available to boaters include satellite and aerial photography. Tools such as Google Earth and Microsoft Bing allow viewing of lakes at various periods over time [13, 52]. By studying lake photography when lake levels are extremely low, boaters can identify potential hazards. The hazards must be fairly large to be identifiable in the photos and accurately assessing the height and elevation of these objects is usually not possible. Photography for drought periods is not always available. Unless the lake is

completely drained, there will likely be large submerged hazards that are not visible in the photography.

Many boaters use online media to communicate information about potential hazards. Most popular lakes will have an unofficial fishing or boating forum(s). Some of the most active forums tend to be fishing related where members discuss angling opportunities and share a variety of lake related information. Some of these posts will be navigational related. The most precise and accurate posts will include screen shots from a digital map and sonar imagery; however, those posts are rare. Often posts of this nature will only give a generalized location and depth, and may employ the use of local slang such as “*I damaged my prop on rocks near party cove*” or “*watch out for the brush piles by the magic crappie tree*”[1, 10, 11].

For detection of submerged objects, boaters do have a selection of recreational grade sonar units for a modest purchase price. These units are marketed toward anglers and include side scanning and down looking modes designed specifically to scan down submerged structures such as standing timber, pylons, and boat wrecks that fish tend to school at. The sonar units allow the operator to pinpoint the depth and GPS location of the submerged objects. Operating a sonar unit does take some training and the imagery it produces can be open to misinterpretation. While these units are common amongst recreational fishing boats, most other types of boats are not equipped with them (ski, personal watercraft, wakeboard, sailboat, party barge, etc.) Also this type of sonar application scans directly beneath and off to the sides of the vessel. It is not intended to be used to avoid navigational hazards in front of the boat when underway [9].

An ideal solution and one that this research attempts to prove possible is a map built with information previously collected from commonly available sensor systems, such as hull mounted side scanning sonar, and displays locations and depths of submerged hazards. If implemented for digital media such as a hand held mobile device or an embedded display installed on a vessel, a map of this nature could also account for the lake's current elevation and the vessel's draft. It could also be layered over bathymetric maps. Areas of the lake known to possess or to have a high risk of containing hazards at the given elevation would be indicated as such. Boaters can then make informed navigational decisions.

Chapter 2

BACKGROUND

2.1 Side Scanning Sonar

Side scanning sonars are acoustic sensors and a mature technology that excel at mapping large areas of the seafloor, or in freshwater applications the lake bottom. Typically dual channel, they emanate lobes perpendicular to their course, or track. To provide better track resolution and cover a large amount of lake bottom, the lobe shape is narrow along the track and wide along the cross track. Bursts of acoustic energy also known as pings will travel out and echo off of objects and lake bottom. The strength of the echo is a function of the object's distance, the angle of incidence, and the ensonified material. Assuming constant material and a flat terrain, lake bottom echoes closest to the transducer will be the strongest and have the best resolution [14].

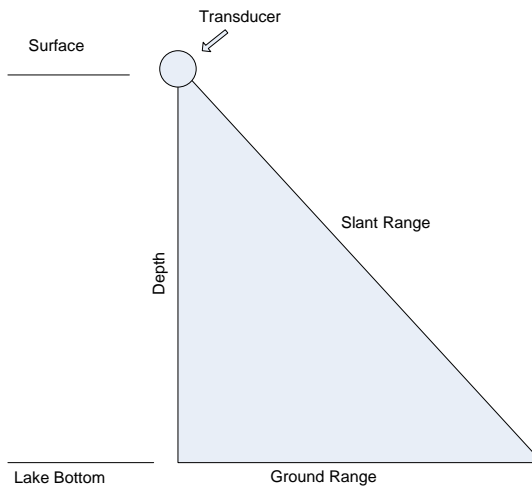


Figure 2.1.1 Sonar Distance Terminology

The sonar system can calculate the distance of objects by measuring the elapsed time from the emanation of a burst of acoustic energy. The distance will have both depth and cross track components as noted in Figure 2.1.1, commonly referred to as slant range distance. It is important to note that the source of the echo's elevation angle within the lobe is ambiguous without further analysis; therefore, the depth and ground range could vary along an arc within the lobe [14]. The red curve in Figure 2.1.2 demonstrates equivalent slant ranges.

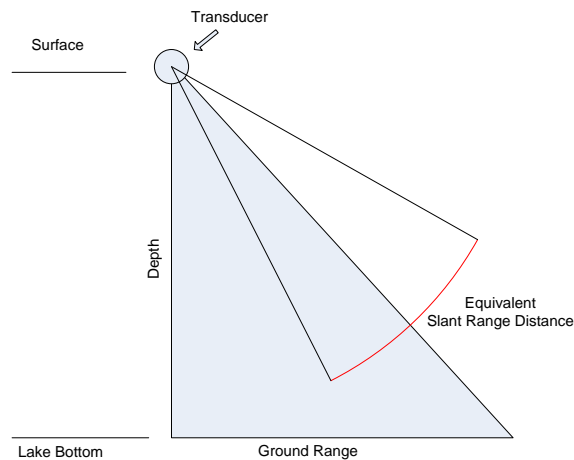


Figure 2.1.2 Equivalent Slant Range

2.2 Side Scanning Sonar Interpretation

Native side scanning display formats present sonar returns in slant range. The vessel's current position is represented at the top center of the display along with the most current sonar returns. As these returns age, their history is moved down the screen. The area of minimum returns in the center of the display represents the water column. As depth increases this area will widen and vice versa. For areas of relatively flat lake bottom and no structure the first returns will be located directly beneath the boat.

Increases in terrain elevation or structures rising out of the terrain will generate stronger returns. Decreases in terrain elevation or areas with an obstructed line of sight to the transducer will generate weak to no returns. Obstructed areas are termed as shadows and often provide geometric clues about the ensonified structure [9, 14, 15].

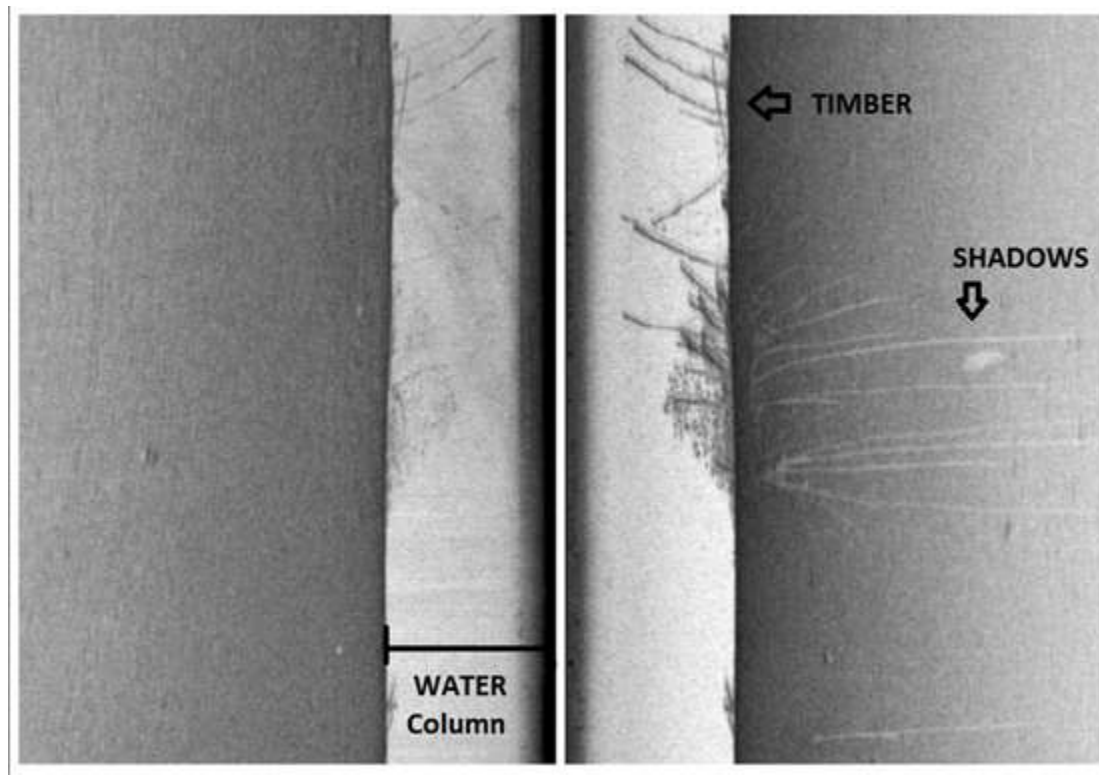


Figure 2.2 – Example Side Scan Imagery

The displayed distance of objects in the water column in Figure 2.2 is the slant range distance from the transducer to the object and not necessarily the distance to the top of the water column. The distance and depth of an object are only the same when the transducer passes directly over the object. The timber at the top of the screen passed almost directly beneath the transducer. This is indicated by the timber being mirrored in both channels and the absence of shadows. By looking at the shadows, the timber about

halfway down the screen is approximately the same depth and off to the starboard side of where the transducer passed.

2.3 Recreational Side Scanning Sonars

Side scanning sonars have been used by various research organizations, the United States Navy, and other navies of the world for over fifty years. However, the specialized nature and cost of this type of sensor has historically precluded it from many potential uses, particularly in freshwater. This changed in 2005 when the first recreational grade side scanning sonar system became available. Today this type of sensor is commonly found installed on recreational angling vessels. Recreational grade side scanning sonar does present opportunity to economically create high resolution maps of aquatic environments; however, for automated processing they also present some unique challenges as compared to their more specialized counterparts [31, 32, 33].

The first challenge that must be addressed is how to capture the side scanning video and provide it in a digital format along with other pertinent sensor information to an automated algorithm. Military and commercial sonar equipped platforms have standardized data busses such as MIL-STD-1553, STANAG 3838, and numerous ARINC standards that onboard sensor systems are required to conform and interface with. Most of these bus technologies are not found on recreational fishing vessels. Interfaces for Ethernet, RS-232, NTSC, and removable flash disks are often available; however, with the exception of NTSC video, specific data structures utilized with these digital formats are considered proprietary information. They are not required to conform to industry data

standards such as extended Triton Format (.XTF) [50], and the manufacturer may or may not be willing to share them.

The second challenge deals with the location of the transducer. Recreational grade side scanning sonar transducers are usually mounted directly onto the vessel's transom as opposed to a towfish [9, 49]. The advantages of this location include the convenience of not having to deploy a towfish as well the ability to use the sonar in locations that have snagging hazards for a towed device. The major disadvantage of a transom mounted transducer is the potential for interference from the vessel's hull, accessories, and engine. This interference can manifest itself as artifacts in the sonar imagery that must be accounted for to prevent false detects with any type of automated interpretation.

A third challenge with recreational grade sonar is that the manufacturers do not document and publish all pertinent technical information with regard to its sensing capabilities, such as lobe shape specifics [9]. These types of details can fall into the realm of product trade secrets, and companies will not typically share this type of information without a non-disclosure agreement (NDA). This can be problematic when attempting to perform a detailed interpretation of the imagery or when attempting to build a model of the sonar. Educated inferences or additional experimentation will most likely be required. This is evident in numerous threads in online support forums for these sensors [37].

2.4 Automated Interpretation of Side Scan Sonar Imagery

Automated interpretation of sonar imagery has continued to be an active area of research since the 1990's. It is also commonly referred to as computer aided detection (CAD) and computer aided classification (CAC) and has a variety of targeted applications including seabed surveys, oil and gas pipeline monitoring, and specific target recognition for naval mine hunting. Most approaches entail noise reduction preprocessing and some form of highlight area and shadow analysis to derive sea floor texture or geometric properties of objects protruding from the sea floor or suspended in the water column. The algorithms employed in CAD/CAC represent a subset of much larger fields of study in machine learning, computer vision, and image processing. Both supervised and unsupervised techniques are encompassed [15, 16, 30, 44].

Most CAD/CAC algorithms are targeted toward analyzing sea floor returns, and their first step is to determine which pixels are highlight, shadow, and sea bottom reverberation. This type of processing is referred to as segmentation. The simplest form of segmentation is to apply a threshold at a given greyscale value. To break out all three classes of pixels, two threshold values would be used.

Choosing threshold values can prove to be challenging. The first issue is that sea bottom imagery tends to be fairly noisy. The second issue is that sea bottom pixel brightness is a function of distance and depth. Building a histogram and normalizing the pixel brightness can help counter this effect, but does not address noise very well. To address this problem a more sophisticated approach is introduced by Guillaudeux et al. [45] built upon fuzzy logic and an expert system of rules. Segmentation is further

improved by the employment of Markov Random Fields to model spatial dependencies between pixels [46, 47].

Existing CAD/CAC publications are targeted toward finding man-made targets in a sea environment or classifying various types of sea beds. Most sea environment is much deeper than that found in freshwater impoundments, and the target's geometry and location within the water column are also very different. In freshwater impoundments, targets include trees, pylons, large rocks, and chunks of concrete that often come close to the water's surface. As such many of the CAD/CAC algorithms presented in published papers may not be applicable without some type of adaptation.

2.5 Occupancy Grids

One of the earliest works to explore gridded probability mapping for obstacle avoidance was published by Moravec and Elfes in 1985, "High Resolution Maps from Wide Angle Sonar" [21]. Moravec et al. describe an approach using wide angle sonar sensors to build maps for robot navigation. The robot is on a level floor inside a laboratory and uses an array of sonars to detect navigational obstructions around it. Each individual sonar reading only contains a small amount of data about the robot's surroundings, but this information is projected onto several two dimensional grids. As the robot moves around, more data is collected, and the map improves.

Due to the choice of using a wide angle sonar, the echoes in this experiment have a similar ambiguity to those produced by a side scanning sonar. Targets detected in this wide beam angle could fall into a range of azimuth and distance values. Moravec et al. characterize this situation as "somewhere OCCUPIED" [21]. The authors make a single

target assumption and divide the probability of occupation across all potential grid points. In other words, the combination of all the probabilities across the grid points equals one. It is worth noting that the probability distribution is not handled symmetrically for empty areas whereas each point is considered independently based on range and angular distance of the cell.

The algorithm presented maintains three sets of grids that are used to calculate values into a final map grid. The first two hold the occupied and unoccupied probabilities. The values in each grid are then summed against each other with the larger value ultimately determining if the final grid location is considered occupied or not.

In 1988 Elfes et al. published a continuation to this previous work, "Integration of sonar and stereo range data using a grid-based representation" [22]. A new framework summarized in Figure 2.5 was presented that enables fusion of different types of sensors. The sensor readings are processed by specific spatial interpretation and detection uncertainty modeling before being combined with positional information. After the sensor reading has been localized it is then fused with other information derived from the same type of sensor. Bayesian mechanics are then applied to fuse the sensor type maps, and threshold decision rules are used to create the final map.

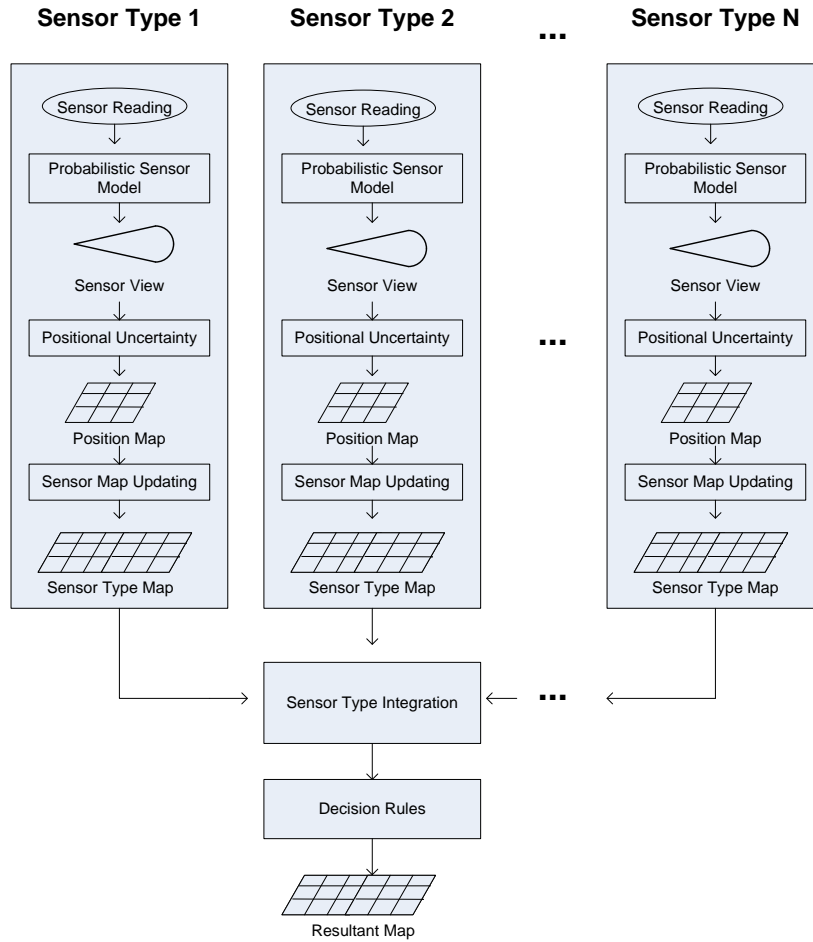


Figure 2.5 – Sensor Integration Framework [22]

Another advance presented is the development of a Bayesian model for updating probabilities in the occupancy grids. Starting with Bayes' Theorem:

$$P(s_i|e) = \frac{P(e|s_i)P(s_i)}{\sum_j^n P(e|s_j)P(s_j)} \quad [23]$$

Table 2.5.1 - Bayes' Theorem Parameters

s	Set of disjoint states
n	Number of states
$P(s_i)$	Probability of being in state s_i
e	Evidence
$P(e s_i)$	Probability of e being present in state s_i
$P(s_i e)$	Probability of system being in state i , providing e

Elfes et al then derive the occupancy update model:

$$P(OCC|R) = \frac{P(R|OCC) P(OCC)}{P(R|OCC)P(OCC)+(1-P(R|OCC))(1-P(OCC))} \quad [22]$$

Table 2.5.2 – Occupancy Update Model

$P(OCC)$	Current Probability of grid point being occupied
$P(OCC/R)$	Probability of grid point being occupied given new sensor reading
R	Sensor Reading (Evidence)
$P(R/OCC)$	Probability of the Sensor Model given R

The update model is implemented by initializing all grid points to probability of occupation ($P(OCC)$) to 0.5 (UNKNOWN). If more is known about the environment before starting exploration, the grid can be initialized differently. As new sensor readings are received, grid points are updated by solving for $P(OCC|R)$. Grid points with a higher confidence of being occupied will have $P(OCC)$ approaching 1, and those that are likely empty will have values approaching 0.

One of the major advantages of the Bayesian approach is that it is both mathematically commutative and associative; therefore, multi sensor systems may have their readings applied in any order.

In a manner similar to the 1985 publication, the new framework and update model are then implemented for use with the Neptune mobile robot that is equipped with a pair of forward mounted cameras in addition to the original wide angle sonar array. The updated system is then used to create maps in an indoor laboratory office environment [22].

Elfes, Matthies, and Moravec laid a foundation with these two publications that continued to be enhanced and expounded upon through the 1990's and into the new millennium. Table 2.5.3 provides a short list of applicable research in chronological order.

Table 2.5.3 – Additional Works in Gridded Occupancy Mapping

1995	Real-time map refinement by fusing sonar and active stereo-vision [24]
1997	Improved Occupancy Grids for Map Building [25]
1997	Probabilistic octree modeling of a 3D dynamic environment [26]
2009	Bayesian Occupancy grid Filter for dynamic environments using prior map knowledge[27]
2015	Robust and Efficient Multirobot 3-D Mapping Merging With Octree-Based Occupancy Grids [28]

2.6 Transforming Coordinate Systems

Gridded mapping approaches utilize a Cartesian coordinate system denoted in cells or linear distances from a point of reference as x and y . As shown in Figure 2.6, GPS enabled sensor systems express location as geodetic angles about a spheroid in latitude and longitude. To transform coordinate systems from a spheroid to a flat plane there exists a library of popular projections. None of which are best for all cases, and all of them induce distortions. Depending on the map location, size, and objectives different map projections will be more ideal [18].

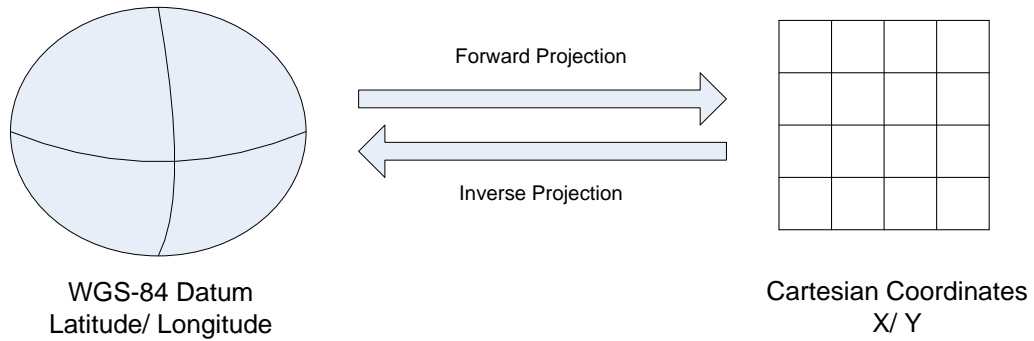


Figure 2.6 – Projection Transforms

One such projection is known as Lambert Conformal Conic (LCC) was published by Johann Heinrich Lambert, an Alsatian mathematician and cartographer in 1772 [19]. It is currently used today in numerous applications including aeronautical, a number of states in the U.S. State Plane System of 1983, including the state of Texas, and marine mapping applications [17]. The transform is performed by placing a cone over the earth, defining a north and south parallel, and then projecting the earth’s surface onto the cone.

Table 2.6.1 - LCC Transform Equations Parameters

a	Semi major axis of reference ellipsoid
f	Ellipsoidal flattening
ϕ_1	Latitude of first standard parallel
ϕ_2	Latitude of the second parallel
ϕ_0	Latitude of the origin
λ_0	Longitude of the origin
Y_f	False Northing
X_f	False Easting
ϕ_i	Input Latitude (to be forward projected)
λ_i	Input Longitude (to be forward projected)
Y_c	Computed Northing
X_c	Computed Easting
ϕ_c	Computed Latitude
λ_c	Computed Longitude
Y_i	Input Northing (to be inverse projected)

X_i	Input Easting (to be inverse projected)
m_i	Temporary Variable

The algebraic expressions shown in Tables 2.6.1 and 2.6.2 should be solved when the map area is defined in bounding parallels, and an origin has been specified. To avoid the negative easting and northing offsets when performing forward projections, it may be desirable to specify non-zero false northing and easting values. Once these constants are set, they should not be altered for the given projection.

Table 2.6.2 - LCC Transform Constants [19]

$m_1 = \frac{\cos \phi_1}{\sqrt{1 - e^2 \sin^2 \phi_1}}$		$m_2 = \frac{\cos \phi_2}{\sqrt{1 - e^2 \sin^2 \phi_2}}$	
$t_0 = \frac{\tan \left[\frac{\pi}{4} - \frac{\phi_0}{2} \right]}{\left(\frac{1 - e \sin \phi_0}{1 + e \sin \phi_0} \right)^{\frac{e}{2}}}$	$t_1 = \frac{\tan \left[\frac{\pi}{4} - \frac{\phi_1}{2} \right]}{\left(\frac{1 - e \sin \phi_1}{1 + e \sin \phi_1} \right)^{\frac{e}{2}}}$	$t_2 = \frac{\tan \left[\frac{\pi}{4} - \frac{\phi_2}{2} \right]}{\left(\frac{1 - e \sin \phi_2}{1 + e \sin \phi_2} \right)^{\frac{e}{2}}}$	
$e = \sqrt{2f - f^2}$ (Eccentricity)			
$n = \frac{\ln m_1 - \ln m_2}{\ln t_1 - \ln t_2}$			
$F = \frac{m_1}{nt_1^n}$			
$\rho_0 = aFt_0^n$			

The algebraic expressions in Table 2.6.3 allow a GPS coordinate expressed as angles in latitude and longitude to be transformed into Cartesian X and Y offset from a point of origin. The false easting and northing value are applied to the final coordinate.

Table 2.6.3 - Forward Projection Algebraic Equations [19]

$t_i = \frac{\tan \left[\frac{\pi}{4} - \frac{\phi_i}{2} \right]}{\left(\frac{1 - e \sin \phi_i}{1 + e \sin \phi_i} \right)^{\frac{e}{2}}}$	$\rho_i = aFt_i^n$	$\gamma = n (\lambda_i - \lambda_0)$
$Y_c = Y_0 + \rho_0 - \rho_i \cos \gamma$		
$X_c = X_0 + \rho_i \sin \gamma$		

The algebraic expressions in Table 2.6.4 allow a Cartesian coordinate expressed as an X and Y offset from a point of origin to be transformed into a GPS location expressed in the angular form of latitude and longitude. False easting and northing offsets are accounted for.

Table 2.6.4 - Inverse Projection Algebraic Equations [19]

$Y' = Y_i - Y_0$	$X' = X_i - X_0$
$\rho' = \sqrt{(X')^2 + (\rho_0 - Y')^2}$	

$t' = \left(\frac{\rho'}{aF}\right)^{\frac{1}{n}}$	$\gamma' = \tan^{-1}\left(\frac{X'}{\rho_0 - Y'}\right)$
$\phi_{t1} = \frac{\pi}{2} - 2 \tan^{-1}(t')$	
$\phi_{t2} = \frac{\pi}{2} - 2 \tan^{-1} \left[t' \left(\frac{1 - e \sin \phi_{t1}}{1 + e \sin \phi_{t1}} \right)^{\frac{e}{2}} \right]$	
$\phi_{t3} = \frac{\pi}{2} - 2 \tan^{-1} \left[t' \left(\frac{1 - e \sin \phi_{t2}}{1 + e \sin \phi_{t2}} \right)^{\frac{e}{2}} \right]$	
$\phi_c = \frac{\pi}{2} - 2 \tan^{-1} \left[t' \left(\frac{1 - e \sin \phi_{t3}}{1 + e \sin \phi_{t3}} \right)^{\frac{e}{2}} \right]$	
$\lambda_c = \frac{\gamma'}{n} + \lambda_0$	

2.7 WGS-84 Datum

To perform projections such as LCC, the Earth's size and shape must be defined. There are several such datums that do this. Sonar data collected in this paper is localized with WGS-84 datum GPS readings. Published in 1984, the World Geodetic System (WGS) 84 models the earth gravimetrically as an oblate spheroid and provides a reference for other Earth centered datum and projections detailed in Table 2.7. [20]

Table 2.7 WGS-84 Datum [20]

a	6378137 meters
f	.0033528

Chapter 3

RELATED WORKS

3.1 “A Bayesian approach to object detection in sidescan sonar” [29]

Calder et al. present a method of CAD/CAC with a Bayesian based approach. Shadow analysis is employed using a supervised algorithm to detect objects protruding from the sea floor. The effectiveness of this approach is highly dependent on having properly trained data for specific targets to be detected. This approach may be too narrow to be used alone to find navigational hazards, but could potentially be run in parallel with other detection methods. Specific hazards of interest such as submerged vehicles could potentially be trained into this approach.

3.2 “A Novel Technique for Mapping Habitat in Navigable Streams Using Low-cost Side Scan Sonar” [31]

Kaeser et al. present a technique in mapping submerged freshwater habitat with low-cost or recreational grade sonar. Sonar imagery is collected and then manually analyzed. Some semi-automated mapping overlay tasks are performed with ArcGIS, but slant range correction and automated imagery analysis tasks are not performed. This work is related because the sonar sensor system employed is almost identical to the one used in this thesis, and Kaeser et al. successfully demonstrate that even though these low-cost sonars are marketed toward recreational activities, the imagery they produce are of sufficient quality for endeavors of a more scientific or professional nature. This grade of sensor system allows studies that would otherwise be too cost prohibitive to accomplish

[31, 32]. Kaeser and Litts continually improved this technique and teach it in training classes for other natural resource professionals [33].

3.3 "Map uncertainties for unmanned underwater vehicle navigation using sidescan sonar" [34]

Guo et al. build upon a gridded Bayesian based framework by creating uncertainty profiles for side scanning sonar systems on unmanned underwater vehicles (UUVs). UUV's are prone to angular deviations in pitch, roll, and yaw. This creates uncertainties as to exact location of a given sonar return. These uncertainties increase with the distance of a given return.

Chapter 4

MODELING AND DESIGN

4.1 Overview

The modeling and software design approach for creating submerged hazard maps is broken into four major phases: 1) collection of sonar traces, 2) sonar imagery analysis, 3) spatial and temporal analysis, and 4) generation of maps.

4.2 Collection of sonar traces

Sonar imagery is collected through the normal use of the sensor on a target lake. The operator should select an area and pilot the vessel to provide sufficient lake bottom coverage at a speed within the sonar's recommended operational range. Environmental conditions will impact the quality of the sonar imagery and its interpretation. During periods of high wind or rapidly rising or falling lake levels, samples should not be taken. The operator will also need to make note of the lake's current elevation level.

In addition to the current lake level, several measurements of how the sonar unit is installed in the vessel must be recorded. Sonar transducer depth and the sonar offset from the GPS receiver should be noted. Depending on how the side scan unit is installed, both channels might not be usable. If this is the case, the operator should note this as well.

The sonar imagery will need to be converted into a digital video format either as a live stream or a standard file format. There are several options available. Most sonar units provide a means to save recordings that can be replayed at a later time either directly on the unit or transferred to a PC. Some units also provide support for an

additional display via an NTSC compliant interface. A scan converter could be used to collect video in this manner.

The following assumptions are made about the collection of video:

- Deviations of vessel heading and course over ground are negligible
- Transducer variance in pitch, roll, and yaw are negligible
- The transducer elevation and lake elevation level are consistent throughout the recording
- The video is collected in a manner that allows displaying all sonar channels and associated readouts for GPS position, course, and depth.
- The pixel resolution is consistent throughout the video.

4.3 Sonar Imagery Analysis

The next step is to process the sonar video and extract GPS coordinates and the slant range distances to any existing hazards. Video and the measurements taken during the sonar trace collection phase are used as inputs to this software process. Computer vision techniques are implemented to interpret the sonar data in a manner similar to that of a human operator.

As the sonar videos are processed, the software will record the GPS receiver location and slant ranges distances of navigational hazards. The software design organization could be summarized as such:

1. Screen Division
 - a. Port and Starboard Channels
 - b. GPS, COG, and Depth Read Outs

2. Optical Character Recognition
 - a. GPS
 - b. Course over ground (COG)
 - c. Depth
3. Sonar Channel Image Processing and CAD
 - a. Rotation
 - b. Histogram Statistics Generation
 - c. Normalization
 - d. Thresholding
 - e. Target Area Segmentation
 - f. Contours
 - g. Geometric Criteria
4. File Output

The C/C++ OpenCV [35] libraries are used to facilitate opening standard video formats and stepping through them frame by frame as well as performing a variety of common image processing techniques.

4.3.1 Screen Division

At the beginning of each frame in the sonar video, the screen is divided into regions. Regions containing data readouts (GPS, COG, Depth) are each identified. Each of the sonar channels is also identified. For simplification of the software design and implementation, the pixel position of all data regions is assumed to be constant throughout all recordings.

4.3.2 Optical Character Recognition

Each of the readouts embedded in the sonar video must be interpreted. Google's open source Tesseract OCR [36] library is used to conduct the optical character recognition (OCR). The API for this library expects the image to be in binary format, so at least a minimum of image processing is required. Depending on font specifics, training data may be required.

4.3.3 Sonar Channel Image Processing and CAD

This part of the software is run twice on each video. The first pass is to collect pixel brightness information and build a histogram. The second pass is to perform the CAD.

4.3.3.1 Histogram Statistics Generation

The segmentation process relies on pixel brightness histogram statistics to account for the gradient in mean pixel intensity with respect to distance and approximation of noise. One option is to skip this step in favor for a constant greyscale threshold; however, expected results would be poor. To construct the histogram, the sonar video(s) is viewed, and the greyscale value of each pixel in the water column is recorded with respect to its distance from the transducer. This information is written to a file and processed in excel or with a statistics package to extract the mean, median, standard deviation, covariance, etc. of each pixel range. Alternatively this information could be handled programmatically in written software as well.

An important assumption is made about the video used to build the histogram. The event of a pixel containing structure as opposed to water is rare.

4.3.3.2 CAD

Each of the image blocks containing the sonar channels is rotated such that the top of the image represents the top of the water column and depth increases as the bottom of the image is approached. This is done to make human observation of the CAD results easier to assess.

The first step is to perform segmentation to identify pixels in the water column that contain structure.

- 1 The value of each pixel in the water column is expressed in terms of standard deviations from the median pixel brightness for its respective depth.
- 2 The median pixel brightness is assumed to be the median echo strength of water as opposed to structure. Noise in the water column is assumed to be Gaussian; therefore, any echo strength less than the median echo strength plus three standard deviations is considered water.
- 3 Only pixels that contain a return strength that are at least three standard deviations from the mean for a given depth will be considered occupied with a potential hazard.
- 4 To assist contouring used in the next step, all pixels at the current water depth are set to a minimum return strength. Also pixels at the history maximum point are also set to a minimum return strength.
- 5 Thresholding is then applied to create a binary image of occupied and unoccupied pixels.

The second step is to apply contouring to the binary image and draw a bounding box around each contour. To prevent older sonar histories from generating automated detects, any box containing points beyond the maximum history point is not processed. Occupied pixel areas that meet minimum size requirements are considered detected hazards. The top pixel(s) in the hazard contour are used in the calculation of slant range distance.

Geometric criteria:

- Must protrude at least two feet from the lake bottom.
- Must be at least four feet in height if within the top four feet of the water column.
- Must be at least four pixels deep in history

4.3.4 File Output

Each frame analyzed in the sonar video generates a record that contains a GPS location, the associated depth, COG, the slant range distance of hazards detected in either channel, the current lake elevation, and the sonar frequency mode. This data is stored in a text file for future spatial and temporal analysis.

4.4 Spatial and Temporal Analysis

Each of the sonar records is read and processed spatially. Lake elevation levels over time are also accounted for. GPS coordinates are transformed into a Cartesian oriented grid cell location. Specific attributes of the sonar sensor are modeled such that probability profiles may be projected onto the gridded map. With each sonar record, the probability of a hazard existing at certain elevations at the respective grid points is updated. As reinforcing data is collected, the confidence of the map improves. Given

the lake's current elevation and a vessel draft, the final generated maps identify areas of the lake that have a high probability of containing hazards that could threaten navigation.

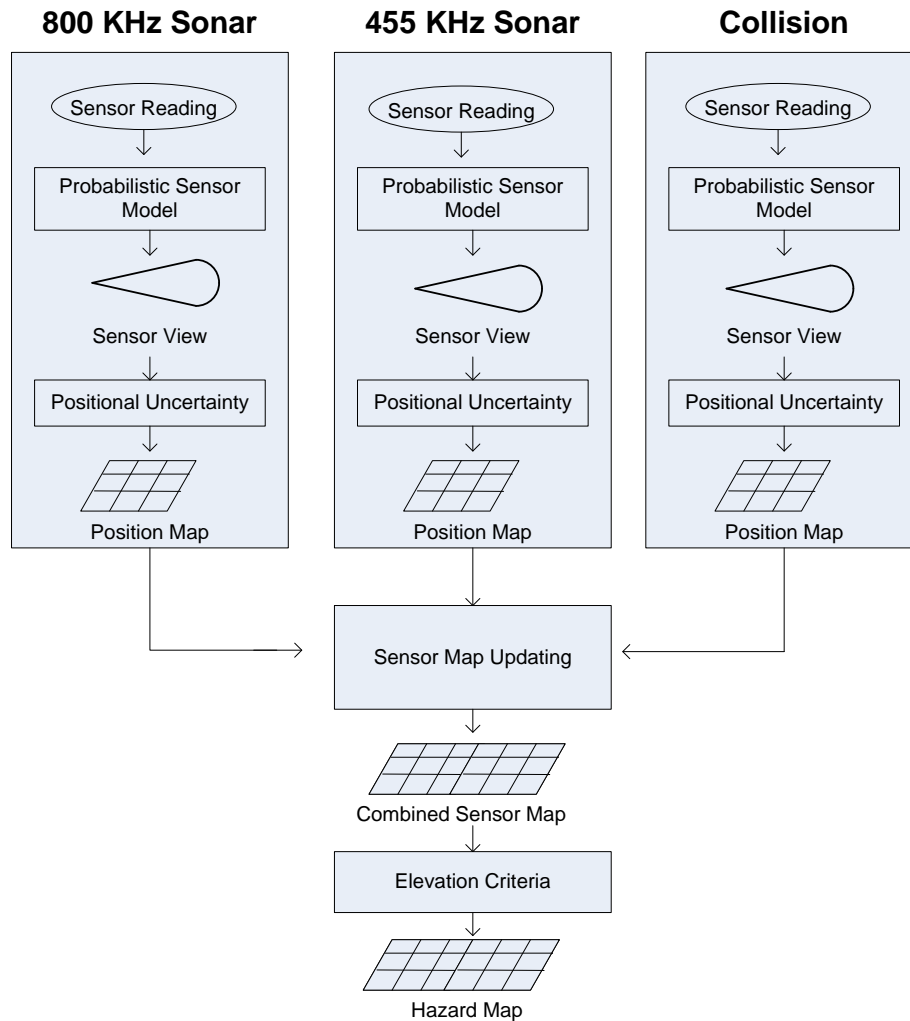


Figure 4.4 – Sensor Integration Approach

Borrowing from Elfes et al. [22] the sensor integration approach is outlined in Figure 4.4. Probabilistic sensor models are created for both of the frequency modes supported by the side scanning sonar selected for this study. Also, the hull of the boat is considered a collision sensor. Locational uncertainty of the boat is also accounted for when fusing the sensor data. After all of the sensor data has been processed, lake level

elevation criteria are applied to generate a hazard map. By altering the elevation criteria, hazard maps for different lake levels are generated.

The software organization is summarized below.

1. File Input
2. Projection Transformation Class
3. Probabilistic Sensor Models
4. Positional Uncertainty Model
5. Gridded Map update
6. Elevation Specific Hazard Mapping

4.4.1 File Input

All file output data from the prior image processing phase of processing outlined in chapter 4.3 is parsed in. The data files should represent a comprehensive collection of imagery processing from all the sonar videos. Care should be taken not to accidentally duplicate any of this data as it would be interpreted as multiple sensor readings and possible skew the final probability map.

4.4.2 Projection Transformation Class

Before any of the imagery results can be populated on the gridded map, the GPS coordinate are transformed into a Cartesian form. This is accomplished using a Lambert Conformal Conic (LCC) projection. This part of the software has a high potential for reuse on future mapping or remote sensing projects. As such care is taken to produce a C++ class that promotes reusability.

LCC
-initialized : bool
+getLL() +getXY()

Figure 4.4.2 – LCC Class UML

The above UML is simplified for presentation purposes and omits all of the necessary projection parameters. The implementation needs to include them, but this is still a relatively simple class that will be initialized with a datum, bounding parallels, origin, and false offsets. For this project that datum is WGS-84. The other parameters are determined by defining the study area. After initialization the forward and inverse methods, **getXY()** and **getLL()** respectively, are invoked to perform the required projection.

4.4.3 Probabilistic Sensor Models

This model defines the probability profile for the sensor. Given the existence of a hazard or lack thereof, bathymetry/depth, and the frequency mode, the model generates a probability hazard presence for each affected grid point.

To determine the probable location of a hazard given a range, the beam angles for the side scanning sonar must be defined. The definition used for this module is derived from the manufacturer’s published specifications [9]. The beam width of the 800 KHz side scanning sonar shown in Figure 4.4.3.1 is modeled as being 55 degrees with the top of the lobe being positioned 25 degrees from the horizontal plane of the transducer. The lower frequency 455 KHz mode shown in Figure 4.4.3.2 is modeled with a much larger lobe with a beam width of 84 degrees and no offset from the horizontal plane of the transducer. Any hazard detected at a given slant range could be located in cross track

range and elevation along a curve in the grey areas of the figures depicted below. An argument can be made that for the intended depths and ranges of operation in freshwater lakes the blind area directly beneath the vessel should be modeled smaller [37].

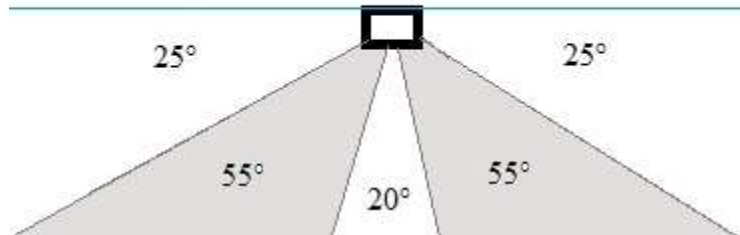


Figure 4.4.3.1 – 800 KHz Sonar Sensor Model [9]

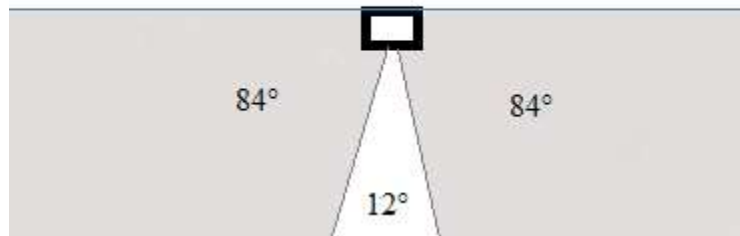


Figure 4.4.3.2 – 455 KHz Sonar Sensor Model [9]

In addition to the sonar sensors, the hull of the boat is considered a collision or contact sensor. It is modeled as protruding 1 foot into the water column and being six feet wide as denoted in Figure 4.4.3.3. So long as the operator does not note a collision with a submerged object taking place, this area is modeled with 100% probability as being empty of hazards. This will be slightly diminished with positional uncertainty.

1 ft x 6 ft

Figure 4.4.3.3 – Collision Sensor Model

4.4.4 Positional Uncertainty Model

Localization is accomplished by using an enhanced GPS that is part of the Humminbird® sensor system. The GPS status readouts while on area lakes claims an accuracy of 3 ft. No additional specifications are provided. Positional uncertainty is modeled as a Gaussian distribution with a standard deviation of $\sigma = 1$ ft. This has the effect of blurring the probability profiles slightly. Uncertainty of yaw, pitch, and roll are assumed to be negligible.

4.4.5 Gridded Map Update

The combined result of the probabilistic sensor models and location uncertainty models are added to the three dimensional lake map grid. Every sensor reading in the input file is stepped through and likewise has its hazard probability results added to the grid.

4.4.6 Elevation Specific Hazard Map

After all of the sensor readings are processed, generation of two dimensional lake elevation specific maps is performed. Given a specific elevation criteria, the three dimensional grid of hazard probabilities is intersected at the respective point on the elevation plane. All grids at or above the specific elevation have their hazard probabilities summed to generate the map. The grid is traversed, and any point with

probable hazards beyond the determined thresholds undergoes an inverse projection back to GPS coordinates and is written out to a comma delimited text file. This process is repeated for additional elevations.

4.5 Generation of maps

After the navigational hazards have been identified and recorded in comma delimited files, they are ready to be imported into maps. There are many ways this can be accomplished. For this research, QGIS [38] is used to overlay the hazards on satellite or aerial photography. The probability value for each hazard location is color encoded to provide more information.

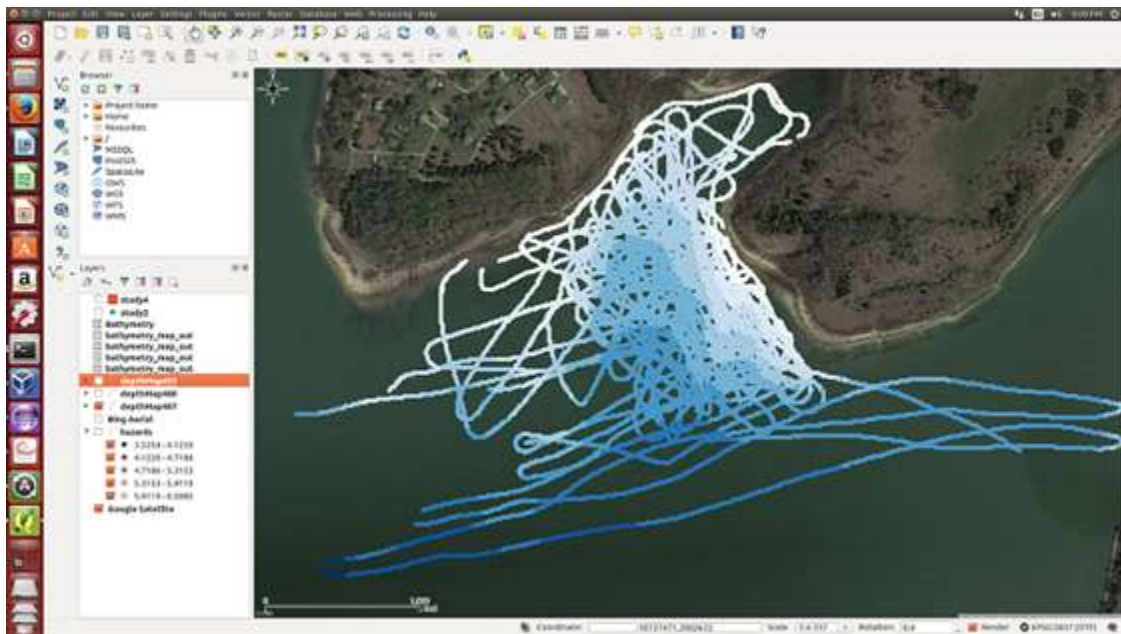


Figure 4.5 – QGIS Project Screenshot

SONAR COLLECTION METHODOLOGY

5.1 Sonar Imagery Collection Parameters

Sonar video is collected with a Humminbird® 889c SI multi-beam sidescanning sonar sensor system at the designated study area on Lake Lavon, Collin County, Texas between the months of February and May 2015. The sonar is installed on an aluminum 17ft deep V recreational fishing vessel as shown in Figure 5.1. The transducer is mounted 8 ft directly behind the GPS receiver on the starboard side of the transom and six inches below the water line. All video is collected while the boat is powered by the aft outboard engine traveling within recommended operational guidelines of speeds ranging from 2 – 6 mph [9].

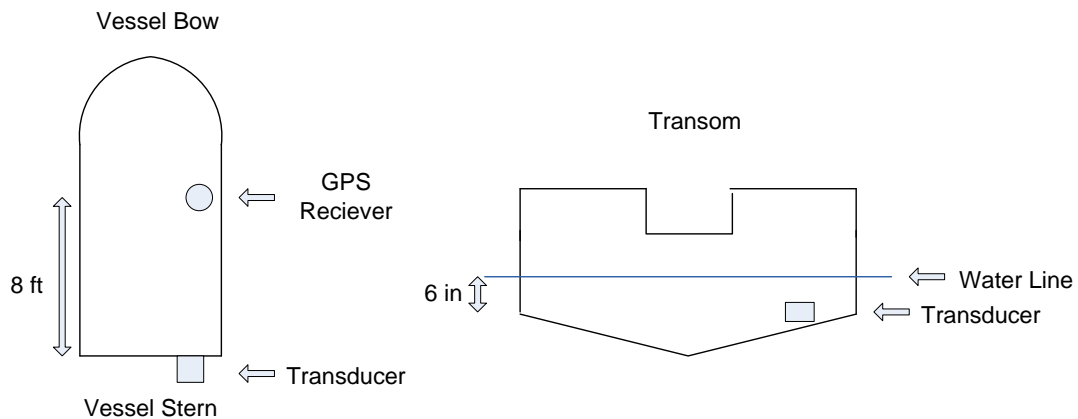


Figure 5.1 – Sonar Installation Parameters

When recording sonar data, the vessel is driven back and forth across the designated study area in a relatively steady course. Care is taken to avoid visible obstacles such as trees. Minor speed adjustments and engine propeller tilts are performed as required for

safety purposes occasionally throughout the recordings. These adjustments do impact sonar returns at the top of the water column on the port sonar channel. All video is saved on removable flash modules in a proprietary Humminbird® binary data format.

5.2 Designated Study Area

The designed study area is a cove on Lake Lavon, Collin County, Texas. This water impoundment was created in 1953 on the east fork of the Trinity River and enlarged in 1975. It is operated by the United States Corps of Engineers and presently covers over 22,000 acres. The full pool level is 492 feet above sea level [39].

Initially, the designated study area on Lake Lavon was the cove containing the power plant on the east side of the lake. Due to heavy rains and the raising elevation level of the lake during the study period, the designated area was moved to a cove further south shown in Figure 5.2.1. The primary reason for moving the study area is it contains a number of known navigational hazards that can be referenced in analysis.

Table 5.2 – LCC Projection Parameters for Study Area

LCC Projection Parameters for Study Area	
Northern Parallel	33.075° N
Southern Parallel	33.030° N
Origin Latitude	33.03175° N
Origin Longitude	96.48240° W
False Easting	-8000 ft
False Northing	-6000 ft



Figure 5.2.1 – Designated Study Area

Aerial Imagery Provided by Microsoft© Bing™ via QGIS Open Layer Plugin. Conforms with Microsoft© Bing™ Terms of Use as Education or Non-Profit Organization usage.

Using Google Earth, older imagery of the lake when it was at a lower elevation is able to be found. The following Figures 5.2.1, 5.2.2, 5.2.3, and 5.2.4 are taken October 18, 2013 when lake elevation was at 479.89 feet above sea level.



Figure 5.2.2 – Designated Study Area on October 18, 2013

By zooming in on the designated test area within Google Earth, potential hazards are identifiable in Figures 5.2.3, 5.2.4, 5.2.5 and 5.2.6. Most of these hazards will become submerged when the lake fills with rain water.



Figure 5.2.3 – Identified Hazards in Designated Study Area North



Figure 5.2.4 – Identified Hazards in Designated Study Area Central



Figure 5.2.5 – Identified Hazards in Designated Study Area South



Figure 5.2.6 – Identified Hazards in Designated Study Area West

It should also be noted that the banks shown in this imagery will not be submerged by lake water until spring of 2015. Live plants, bushes, and small trees will grow for an additional eighteen months before the study takes place.

5.3 Trip Collection Summary

Four sonar collection trips were conducted. Data in the first trip on February 14 is not used in final analysis because it was taken outside the study area. The elevation level of the lake on each of the trips is noted in Table 5.3. The following path summaries are created by extracting GPS location via OCR from the applicable sonar video and plotted over satellite imagery in Figures 5.3.1, 5.3.2, 5.3.3, and 5.3.4. In addition to acoustic and GPS sensor readings, it should also be noted that the vessel used to collect samples did not collide or come into contact with any hazards. The vessel draft is 14” and can be considered a collision sensor in modeling.

Aerial Imagery Provided by Microsoft© Bing™ via QGIS Open Layer Plugin.
Conforms with Microsoft© Bing™ Terms of Use (TOU) as Education or Non-Profit Organization usage.

Table 5.3 – Study Area Lake Levels

Date	Lake Elevation (FT MSL)
April 4, 2015	487.6
April 15,2015	488.69
May 1, 2015	493.25

5.3.1 Data Collection April 4, 2015



Figure 5.3.1 – 800 KHz Sonar Collection Route April 4

5.3.2 Data Collection April 15, 2015



Figure 5.3.2 – 800 KHz Sonar Collection Route April 15

5.3.3 Data Collection May 1, 2015



Figure 5.3.3 – 800 KHz Sonar Collection Route May 1



Figure 5.3.4 – 455 KHz Sonar Collection Route May 1

6.1 Sonar Video Capture and Optical Character Recognition

After collecting sonar data, the associated sonar videos were created using two methods. The first was to replay the video in real-time on the Humminbird® control unit with a scan convertor attached to the NTSC output for a second display. The second method was to remove the flash disk that contained the sonar data stored in a proprietary form and copy the data to a PC for conversion. A third party Java based tool called HumViewer [40] was used to make the conversions.

6.1.1 Scan Converted Video

The scan converted video contained a small, but noticeable amount of additional noise when compared to the video displayed on the Humminbird® control unit. Unfortunately, this additional noise created unreliable results for optical character recognition. Specifically the character's 1 and 7 and 3, 5, and 8 were randomly misrecognized for each other. Additional image processing was able to reduce these errors, but was never able to eliminate them. Use of another scan converter model was not investigated. Retraining Tesseract OCR with the noisy font was also not investigated.

6.1.2 HumViewer Converted Video

HumViewer is a third party Java based application targeted for Windows and MAC. It is a method recommended by Humminbird® technical support to view sonar

recordings on a PC. To get it to run on Linux several shell scripts are created. They are included in APPENDIX B USEFUL SCRIPTS.

The videos created with HumViewer did not introduce any visible additional noise. With only a small amount of image processing, Tesseract OCR is able to retrieve the GPS location, depth, and heading information reliably. Another advantage to this technique is that the video can be converted much quicker than real-time. In other words, a twenty minute video can be created in several seconds instead of twenty minutes. A catalog of created video may be found in APPENDIX D CATALOG OF SONAR VIDEOS CREATED.

6.1.3 General Observations

HumViewer provides a number of optional parameters to create movies. These video settings along with general observation about the created video are summarized as follows. Figure 6.1.3 may be viewed for reference.

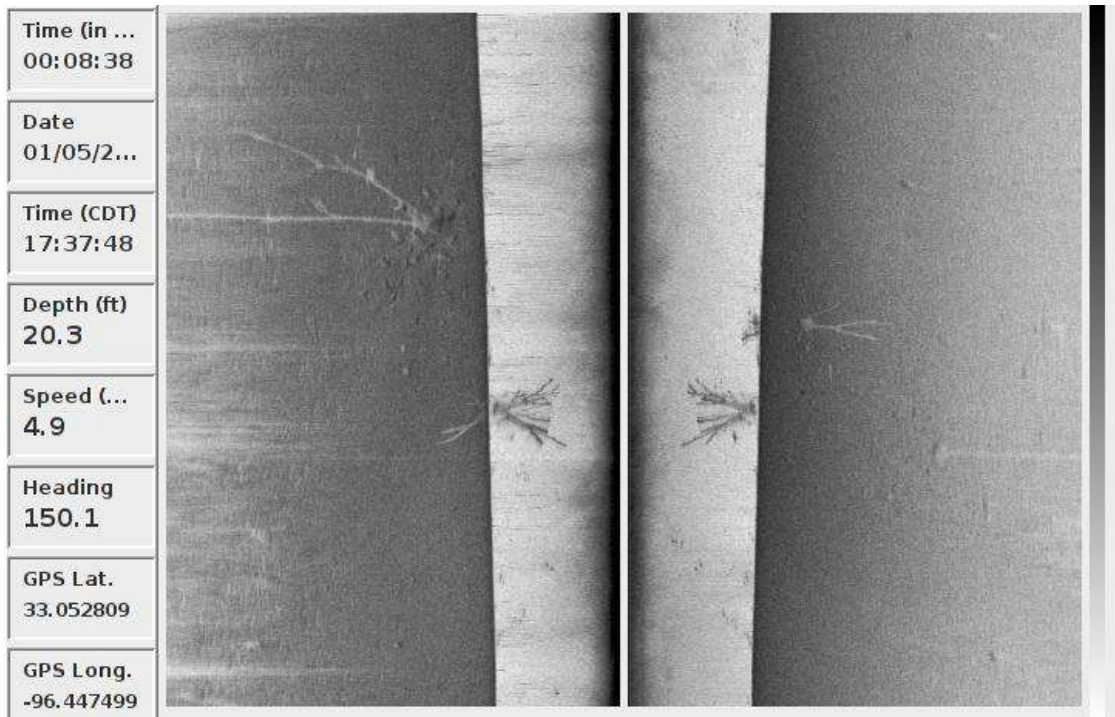


Figure 6.1.3 – Sonar Movie Created With HumViewer

1. Imagery is eight bit gray scale.
2. Maximum range is scaled to sixty six feet.
3. Strongest returns are darkest and shadows are light.
4. Acoustic noise at the top of the port channel is more prevalent than the starboard channel.
5. Overall pixel brightness is darkest at the top of the water column and fades until an object or the lake bottom is encountered.
6. Overall pixel brightness of the bottom returns are darkest closest to the water column and fade with distance.
7. Data readouts such as GPS location, course, date, and time are included and displayed down the left side of the movie screen.

6.2 Pixel Brightness Normalization

Attempting to implement a thresholding segmentation yields poor results without normalizing the pixel brightness. A threshold set to eliminate noise at the top of the water column also eliminates strong reverberations at lower depths, and the CAD misses many structures. A threshold set to detect structures at lower depth triggers many false detects from noise higher in the water column. After normalizing the pixel brightness results are much improved.

After analyzing the brightness distribution for each of the collection sets, it is found that they do differ slightly. Best results are achieved by using the normalization specific to the collection date. Environmental conditions such as water temperature may be a potential cause for changes on the different dates. Pixel brightness distribution statistics for April 4, 2015 are shown in Figure 6.2. The remaining charts are available in **APPENDIX C PIXEL BRIGHTNESS DISTRIBUTIONS.**

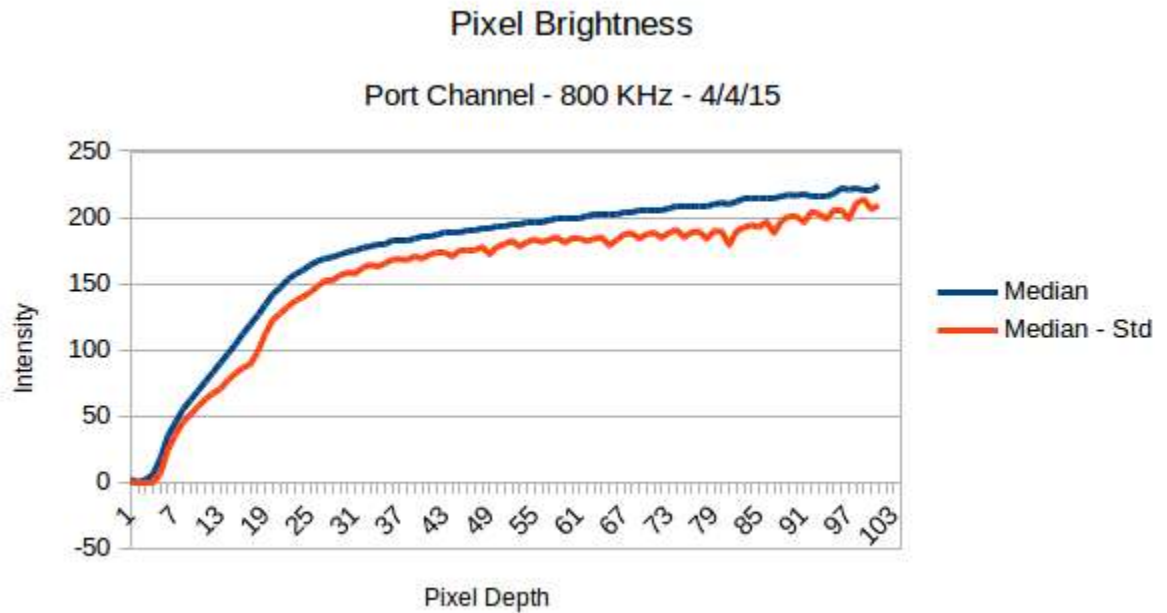


Figure 6.2 - Pixel Brightness Histogram Statistics

6.3 CAD Results

The unsupervised CAD implementation is able to identify most hazards in the water column. However, there are some false alarms, and occasionally the algorithm measures a hazard further away than intended. Figures 6.3.1, 6.3.2, 6.3.3, 6.3.4, and 6.3.5 form a representative sample of CAD results.



Figure 6.3.1 – CAD Results Too Far

In Figure 6.3.1 CAD identifies the tree but misses most of the branches. The resulting measurement for the tree places it further away than it should be.



Figure 6.3.2 – CAD Correct Example 1

In Figure 6.3.2 CAD correctly measures this hazard.



Figure 6.3.3 – CAD Correct Example 2

In Figure 6.3.3 CAD correctly measures these hazards.



Figure 6.3.4 – CAD False Detection

In Figure 6.3.4 CAD generates a false detection. This may be caused by aquatic life such as schools of fish.



Figure 6.3.5 – CAD Correct Example 3

In Figure 6.3.5 CAD correctly dismisses noise and some artifacts that are not hazards.



Figure 6.3.5 – CAD Misses Part of a Submerged Tree

In Figure 6.3.5 CAD correctly identifies the hazard on the left and right, but it misses the top of the hazard in the middle.

6.4 Bathymetry

The intent of this research is not to generate bathymetric maps. However, during the course of operating the sonar, a large amount of fine resolution bathymetry information was collected. This data provides a useful reference. Figure 6.4 summarizes the collected data.



Figure 6.4 – Summary of Bathymetry Data

Aerial Imagery Provided by Microsoft© Bing™ via QGIS Open Layer Plugin. Conforms with Microsoft© Bing™ Terms of Use (TOU) as Education or Non-Profit Organization usage.

6.5 LCC Projection Class

The LCC class is implemented and uses the study area parameters specified in chapter 5.2 to forward project results of the imagery analysis which included bathymetric information onto a Cartesian grid. After all of the data was loaded, the bathymetry information was inverse projected back into GPS coordinates. QGIS was then utilized to overlay the bathymetry over aerial photography. The results are documented in section 6.4. The location of the bathymetry data correlates with other bathymetric studies of the lake [48], and while not entirely conclusive, it does indicate the LCC implementation is working as expected.

6.6 Slant Range Distance of Identified Hazards

The following are summaries of the identified hazards and their slant range distance from the transducer. Results are overlaid on depth charts that are corrected for the elevation of the lake on the day of collection. The satellite imagery was imagery provided by Google Earth via QGIS Open Layer Plugin.

Table 6.6 – Hazard Identification Key

Color	Value
Dark Red	Hazard within 3 feet
Light Red	Hazard within 6 feet

Orange	Hazard within 9 feet
Yellow	Hazard within 12 feet
White (Circle)	Hazard greater than 12 feet
White (Not Circled)	Water Depth less than 5 feet
Lightest Blue	Water Depth 5 to 10 feet
Light Blue	Water Depth 10 to 15 feet
Blue	Water Depth 15 to 20 feet
Dark Blue	Water Depth 20 to 25 feet
Darkest Blue	Water Depth greater than 25 feet

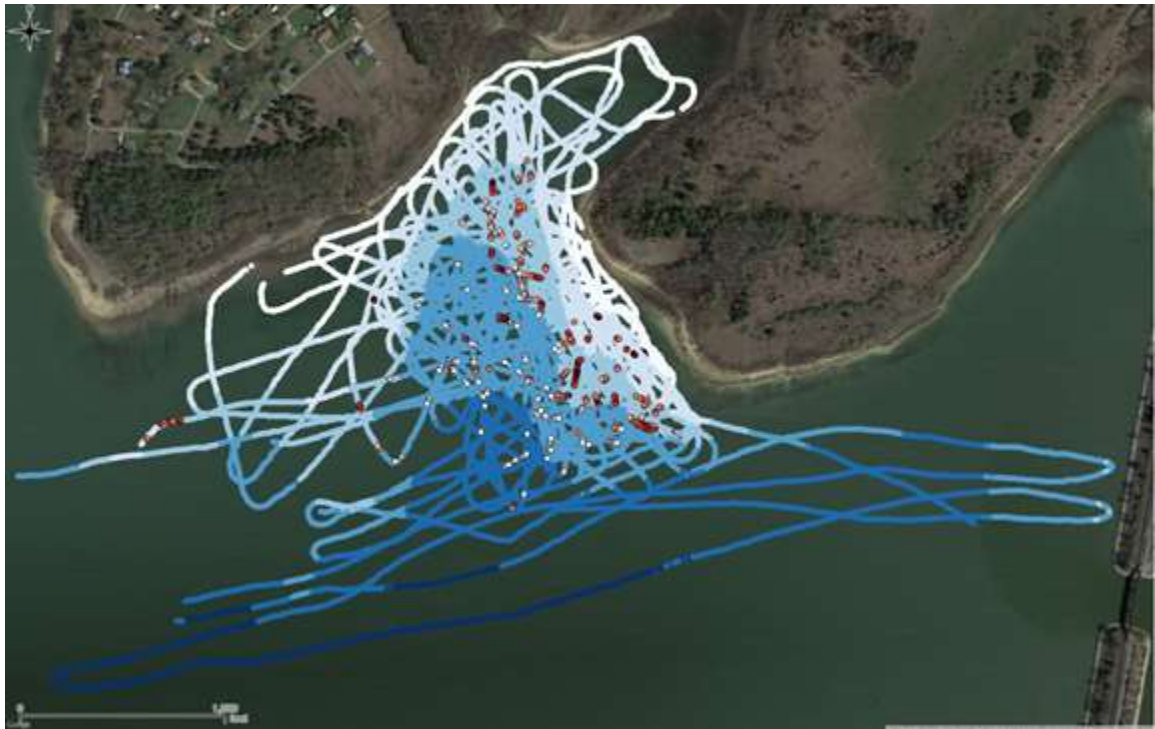


Figure – 6.6.1 Hazards Identified April 4, 2015



Figure – 6.6.2 Hazards Identified April 15, 2015

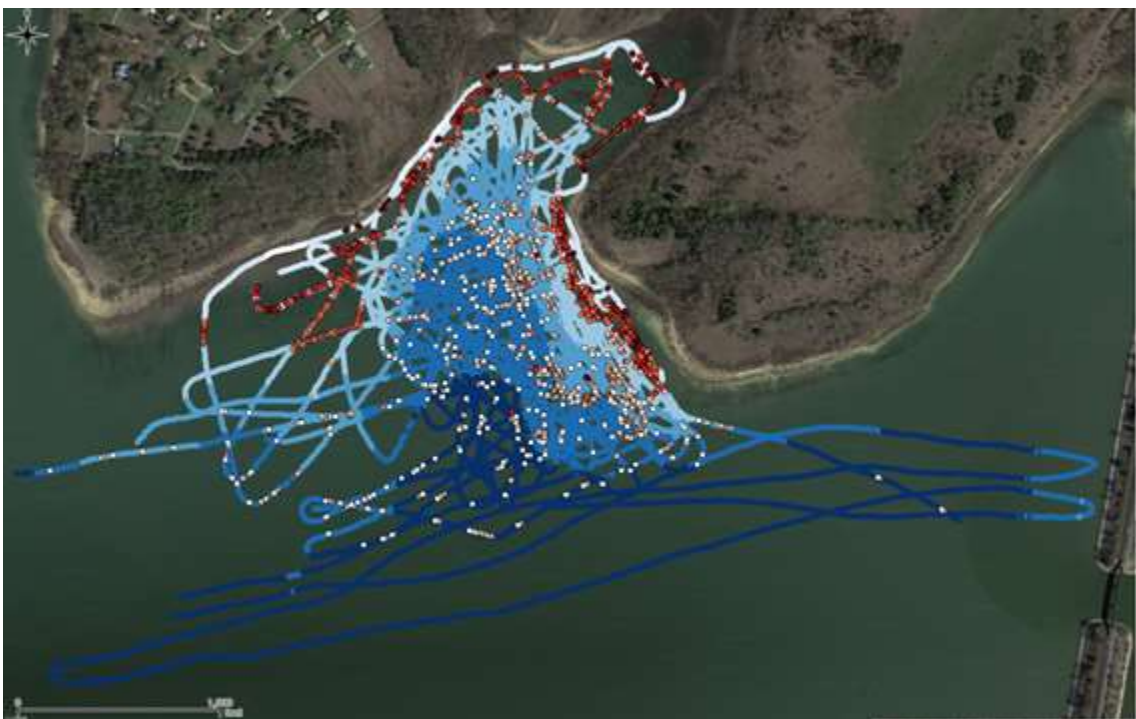


Figure – 6.6.3 Hazards Identified May 1, 2015

6.7 Elevation Hazard Maps

The results of the CAD imagery analysis including the slant range distance to all hazards identified are processed spatially and with respect to the lake level at the date of collection. The gridded Bayesian based model described in chapter 4.4 generates the maps shown in Figures 6.7.1, 6.7.2, and 6.7.3. The red denotes areas where hazards most likely threaten navigation. The pale pink color indicates there is some potential for a hazard to exist at this location. Light blue indicate that sonar data confirms this is a safe part of the lake. Dark blue indicates that boat traffic has safely passed in this location at or below the current lake elevation and sonar has verified that no hazards exist.

The maps compare favorably to hazard areas identified in Figures 5.2.3, 5.2.4, 5.2.5, and 5.2.6 in that the circled areas are recognized as hazardous to navigation. There are additional areas marked as hazardous that need to be investigated to determine if a hazard actually exists.



Figure 6.7.1 - Hazard Map Lake Elevation of 486 Feet

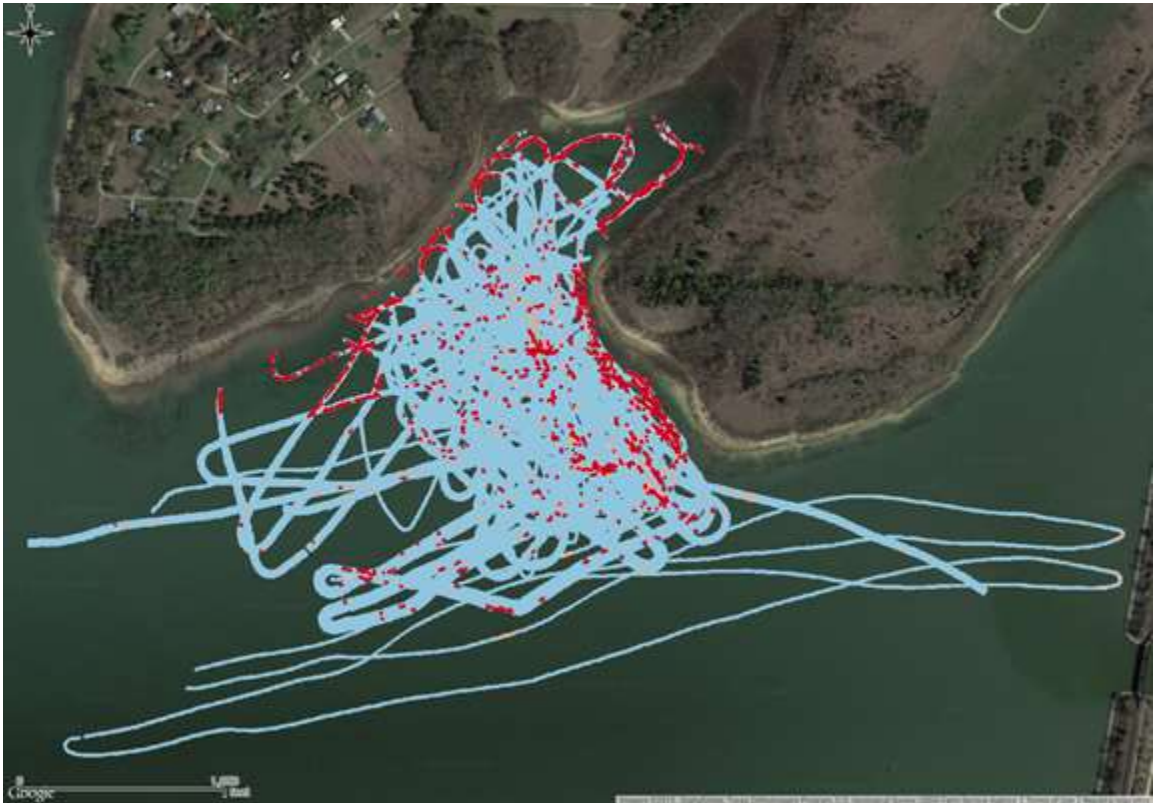


Figure 6.7.2 - Hazard Map Lake Elevation of 489 Feet

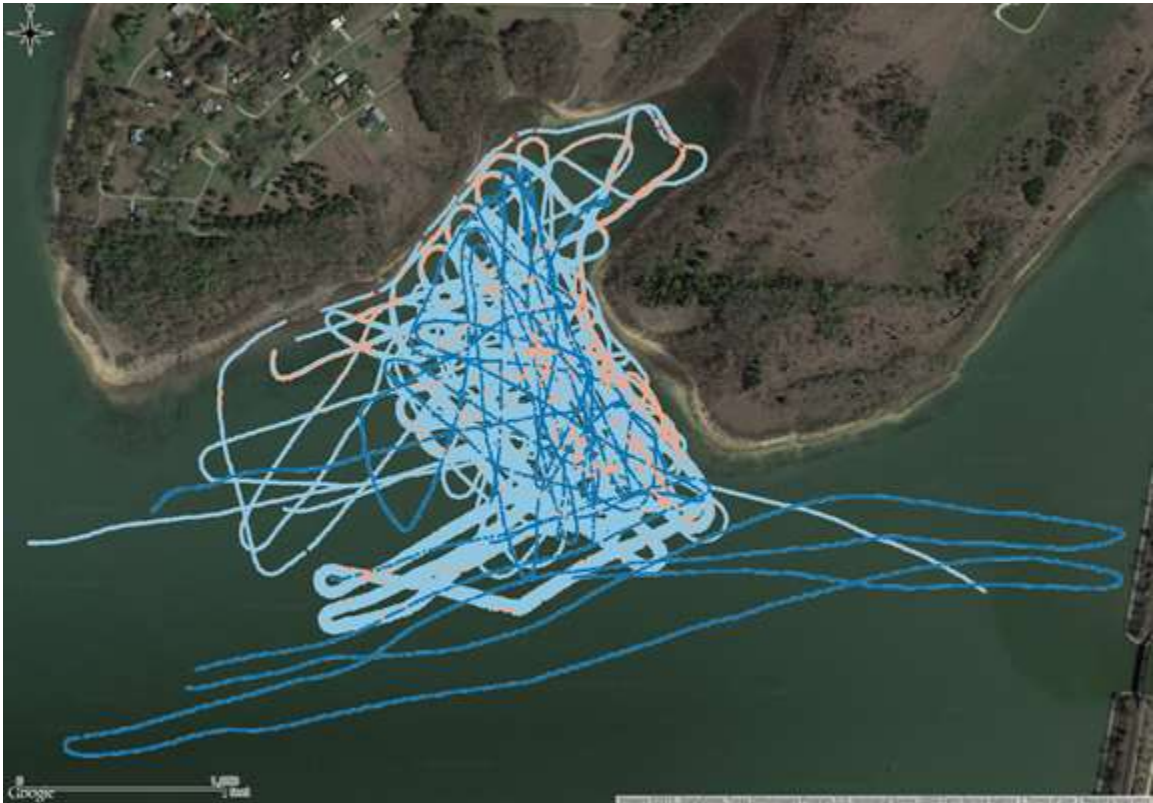


Figure 6.7.3 - Hazard Map Lake Elevation of 493 Feet

6.8 New Hazards at Higher Lake Elevations

The map shown in figure 6.7.3 is deceptive in that it may be interpreted to imply that the lake is safer or contains fewer hazards as the lake level increases. Sonar data cannot be collected in areas shallower than the collection vessel's draft. As water levels increase, there are potentially many unidentified hazards along the new shoreline [51]. While collecting sonar data, the vessel is navigated safety around any hazards protruding out of the water. Unfortunately, this also can prevent hazards from being detected and mapped. There are three known hazards that fall into this category shown in figure 6.8 as red circles.



Figure 6.8 – Additional Hazards

Chapter 7

CONCLUSION AND FUTURE WORK

7.1 Conclusion

Submerged water hazards continue to threaten navigational safety on freshwater impoundments [1 - 8, 51]. There are presently no available maps that provide a comprehensive identification of these obstacle locations; however, automated processing of commonly available sensor systems such as side scanning sonar provides an opportunity to help identify and map these obstacles. Combined with mapping and communication technologies presently available [9 – 13], boaters have the ability to make better informed decisions with regard to submerged obstacle avoidance.

Results from this research are indicative that automated sonar imagery analysis may be employed in the construction of maps containing submerged hazard locations and elevations within a water column. This information can be formatted in a manner that accounts for current lake conditions and targeted to vessels with various drafts. Low cost recreational grade side scanning sonar [9] video is successfully transferred from the target system installed on a vessel to the PC environment for processing. The data format lends itself to being collected at a remote location, tarred, compressed, and transferred over a network if required. With a small amount of image processing, Google's Tesseract OCR [36] is able to successfully interpret all required readouts without any misinterpreted characters. The unsupervised CAD algorithm and software design presented in chapter 4.3 does not flawlessly mark all hazards, but it is able to correctly

identify and measure slant range distance to most of the hazards within the water column. False alarms are generated, but not overwhelming for the given data set.

The approach described in this research has significant limitations. The GPS location of identified hazards is arguably shown to be of sufficient precision and accuracy; however, the same cannot be stated for the elevation of the identified obstacles. Also the CAD identified in chapter 4.3 is shown to underestimate distances to hazards as well generate false detects. The Bayesian gridded mapping approach described in chapter 4.4 may help alleviate problems with the CAD when multiple sonar passes of the given area are available, but has not proven to be able to fully account for these types of errors. While the results demonstrate promise, further study is required to assess and demonstrate a quantifiably reasonable amount of accuracy.

7.2 Benchmarking

The accuracy of generated maps must be quantifiable. Grid location and GPS location comparisons used in past works [21, 22, 43] are not sufficient for the three dimensional nature of submerged hazard mapping. Ideally hazard GPS location and elevation precision and accuracy should be comparable to professional studies such as bathymetric mapping performed by Solis [48]. This would also provide a means to evaluate enhancements made to the CAD techniques and sensor fusion. A set of sonar video representative of the submerged hazards in target lake(s) should be created with known expected results. The video could consist of actual and artificially synthesized footage, but an ideal approach will include actual lake(s). For artificial video, the

expected results could be derived through modeling, but actual lake data will require real world measurement possibly with the use of divers.

7.3 Improved CAD Techniques

The CAD technique implemented in this research differs from other approaches in that it focuses on the water column. While initial results are generally positive, this approach only utilizes a small portion of the sensor data provided. Shadow analysis and pattern recognition can be adapted to further reduce false detections and missed target identification of objects with near cross track distances. It could also be used to identify obstructions with cross track distances that are greater than the present water column depth thus reducing the overall number of passes required to map a given area. Correlation of known bathymetry data and shadow length for a given target could also narrow angular ambiguity and provide a more precise location of a detected hazard. Instead of providing only a slant range for a given hazard detection, this type of CAD could potentially provide a confidence, narrower positional values, and geometrical size describing the detection [15, 30, 34]. Ultimately this could create a more accurate sensor model for sensor fusion.

7.4 Improved Sensor Fusion

Continuing to build from the works of Elfes et al. [21, 22] further experimentation with altering thresholding limits and fusion decision rules is warranted. For example, if a number of contiguous cells are determined to be probabilistically empty could a similar inference be made about the cells above? In the current implementation, all sonar information is projected in chronological order. Since the processing is not performed at

real-time, fusion is not constrained temporally. More accurate maps may be achieved by processing sensor reading in different orderings such as by precision and altering the update model to allow existing grid information to influence the projection of less precise sensor readings. Less precise sensors could then have their projections altered by already known data. Modified update models introduced by later works such as Konolidge's MURIEL approach [25] may also yield better results.

7.5 Fusion with Additional Sensors

In addition to side scanning sonar, other common sonar presentations can be leveraged. This could include azimuth sweeping sonar [43] as well as forward or down looking sonar displays. The unsupervised and supervised techniques developed for shallow freshwater side scanning sonar imagery may be adaptable to support this. Other types of sensor imagery such as satellite and aerial photography in reference for a given lake level could be processed in an automated manner as well. The same could also be done for video or radar imagery taken at lower altitudes either on a small vessel or with an airborne drone. Fusion with sensors above the water level may address the issue outlined in chapter 6.8.

7.6 Automated Collection

The focus of this research targets the use of manned small recreational vessels. Collection techniques could be expanded to include unmanned vehicles. The repetitive nature of this activity lends itself to automation. An ideal group of autonomous vehicles could encompass sensors employed from the spectrum of unmanned platforms including UAV, USV, and UUV [34, 41, 42, 43]. Potentially one operator could oversee a group of

USV's collecting mapping data, and as Manley states "Mowing the lawn never becomes dull for a USV" [42].

APPENDIX A

HARDWARE AND SOFTWARE

The following tools are utilized in conducting this research.

Table A.1 – Hardware Tools

Product	Model
Humminbird® Side Scanning Sonar System	898c SI
Diamond Video Capture	VC500
ASUS Laptop Computer	G73S (8 GB RAM)
DELL Desktop Computer	T3500 (16 GB RAM)
Lowe Deep-V Aluminum 17' Boat	2007 FM 175S
SanDisk Flash	Various 2 to 16 GB

Table A.2 – Software Tools

Product	Version
OpenCV	2.4.8
Tesseract OCR	3.02
QGIS	2.8.0
HumViewer	86
Eclipse	3.7.1, 4.4.1
GNU C/C++ Compiler	4.6.3, 4.8.2
Ubuntu	12.04, 14.04
OpenLayers QGIS Plugin	1.3.6
OpenJDK Runtime Environment	IcedTea 2.5.3

APPENDIX B

USEFUL SCRIPTS

Three useful shell scripts for working with Humviewer and the software created for this research in Ubuntu Linux.

This script will start Humviewer (version 68)

```
startHumviewer.sh
```

```
java -Xms128m -Xmx1024m -cp
```

```
".:/jar/HumViewer.jar:ext/JMF/lib/jmf.jar:ext/JMF/lib/customizer.jar:ext/JMF/lib/mediapl  
ayer.jar:ext/JMF/lib/multiplayer.jar:ext/log4j/log4j-1.2.15.jar:ext/forms-1.3.0/forms-  
1.3.0.jar:." HumViewer.HumViewer
```

This script looks in subdirectories and changes the case of “.IDX” to “.idx”. The extension needs to be lower case for Humviewer to open it.

```
makeLower.sh
```

```
find . -name '*.IDX' -exec sh -c 'a=$(echo "$0" | sed -r "s/([^\.]*)\$/L\1/"); [ "$a" != "$0"  
] && mv "$0" "$a" ' {} \;
```

This script runs imagery analysis on every .mov file in the directory

```
processImagery.sh
```

```
for f in *.mov ; do ./ImageAnalysis "$f" 66 493.25 8 0.5 ; done
```

APPENDIX C

PIXEL BRIGHTNESS DISTRIBUTIONS

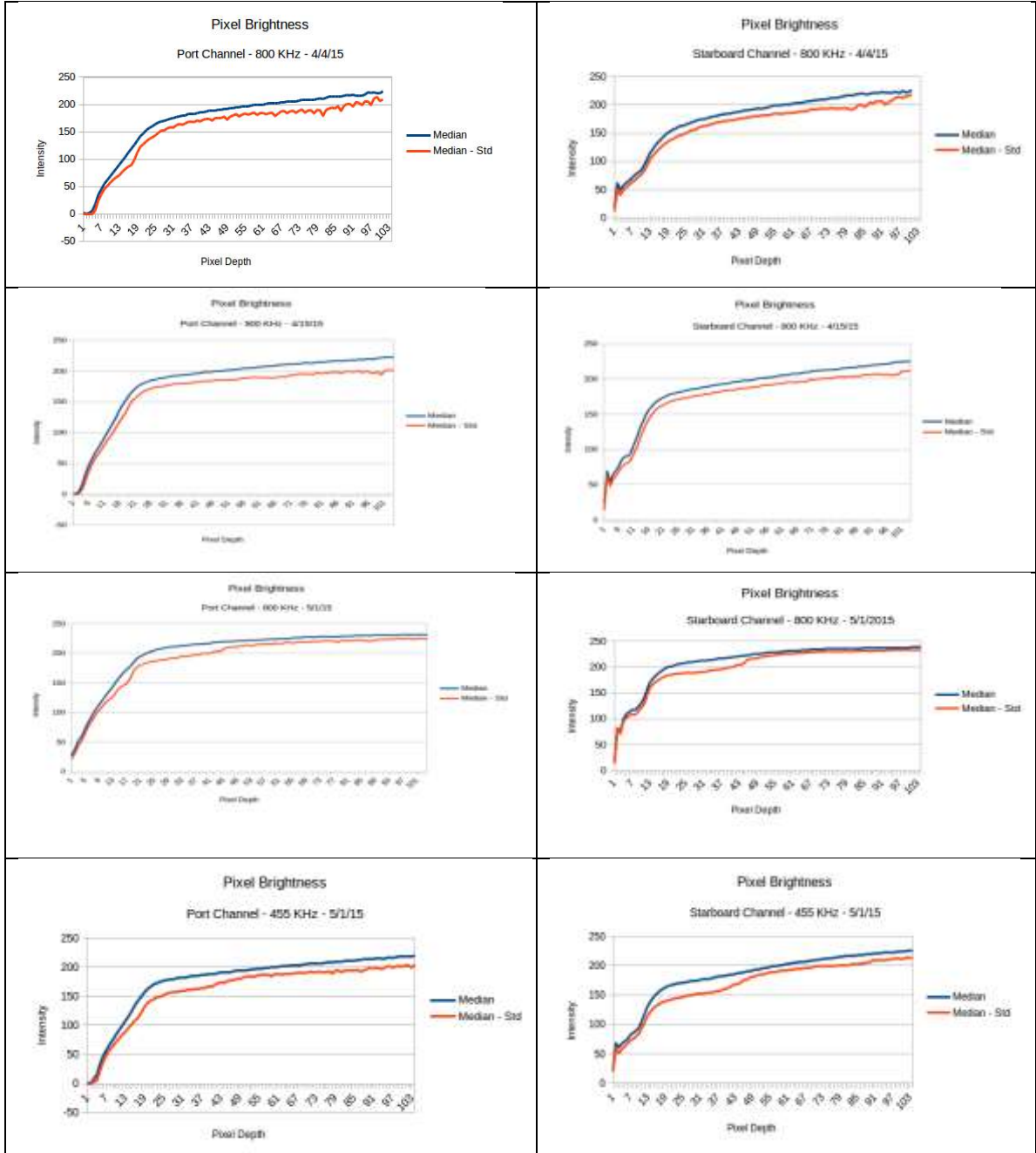


Figure C - Pixel Brightness Histogram Statistics

APPENDIX D

CATALOG OF SONAR VIDEOS CREATED

All sonar videos were created at 1 frame per second. Duration is denoted in minutes:seconds format.

Table D.1 – 800 KHz Sonar Video Recorded April 4, 2015

R12_gray_66.mov	13:27
R13_gray_66.mov	22:48
R14_gray_66.mov	11:08
R15_gray_66.mov	33:36

Table D.2 - 800 KHz Sonar Video Recorded April 15, 2015

R16_gray_66.mov	8:09
R17_gray_66.mov	17:39
R18_gray_66.mov	15:12

Table D.3 – 800 KHz Sonar Video Recorded May 1, 2015

R20_gray_66.mov	11:49
R21_gray_66.mov	4:18
R22_gray_66.mov	6:53
R23_gray_66.mov	8:34
R24_gray_66.mov	8:18
R25_gray_66.mov	10:32
R26_gray_66.mov	8:55
R27_gray_66.mov	9:19
R28_gray_66.mov	15:09
R29_gray_66.mov	9:53
R30_gray_66.mov	15:24
R31_gray_66.mov	11:52
R32_gray_66.mov	12:45

Table D.4 – 455 KHz Sonar Video Recorded May 1, 2015

R19_gray_66.mov	14:26
R33_gray_66.mov	13:04
R34_gray_66.mov	12:12
R35_gray_66.mov	9:09
R36_gray_66.mov	9:03
R37_gray_66.mov	9:32
R38_gray_66.mov	7:59
R39_gray_66.mov	10:16
R40_gray_66.mov	7:25
R41_gray_66.mov	8:08

APPENDIX E

PERMISSION TO USE PHOTOGRAPHY

From: Morris, Phillip Andrew
Sent: Thursday, April 23, 2015 10:27 AM
To: sharon@planetrockwall.com
Subject: Re: Requesting permission to use a photograph from planetrockwall.com

Thank you Sharon.

My thesis involves developing automated mapping technology that can identify and record the depths of navigational hazards such as submerged trees. I'd be happy to give you a copy.

From what I've found, boat collisions with submerged objects are not an uncommon occurrence when lake levels start fluctuating. I hope your friend was able to salvage his boat or at least get back on the water with a new one.

From: Sharon Lewis <sharon@planetrockwall.com>
Sent: Tuesday, April 21, 2015 9:06 AM
To: Morris, Phillip Andrew
Subject: Re: Requesting permission to use a photograph from planetrockwall.com

Hi Phillip,

Yes, sharing the photo with watermark and link to the article is permitted and appreciated.

We know the person who lost the boat. It was a sad day, and surprising to many because he knows the lake and is an experienced member of the sailing community.

If we can see a copy of your thesis that would be great, however, not expected.

On 4/20/2015 11:45 AM, Morris, Phillip Andrew wrote:
Hey Sharon,

I'm a part-time graduate student at SMU (Dallas Campus) working on a master's thesis related to boating hazards. There is a picture worth a million words on your site that I'd like to include.

http://planetrockwall.com/news/article/falling_lake_levels_a_big_problem

The photograph is of the half sunk "Orion" sloop. If you permit it's use, I would include its reference to the article at planetrockwall.com as well as keep the picture's watermark in place.

Thanks
Phillip Morris

APPENDIX F DUAL CHANNEL DETECTION CRITERIA

The following maps are created with a criteria that both channels must simultaneously detect a hazard at the same time. This will happen when the transducer is directly over a large hazard or in between two hazards. The more unlikely event of simultaneous false detects in both channels will also meet this criteria. Implementation of the dual channel criteria is accidental. It is essentially the result of a software bug, but results are interesting so they are placed in Figures F.1, F.2, and F.3.

It should be noted that the bathymetric data in Figures F.2 and F.3 are swapped. The bathymetry shown in F.2 is from May 1 and vice versa. Since the bathymetric overlay is only for reference the maps were not regenerated.



Figure F.1 – Dual Channel Hazards Identified April 4, 2015

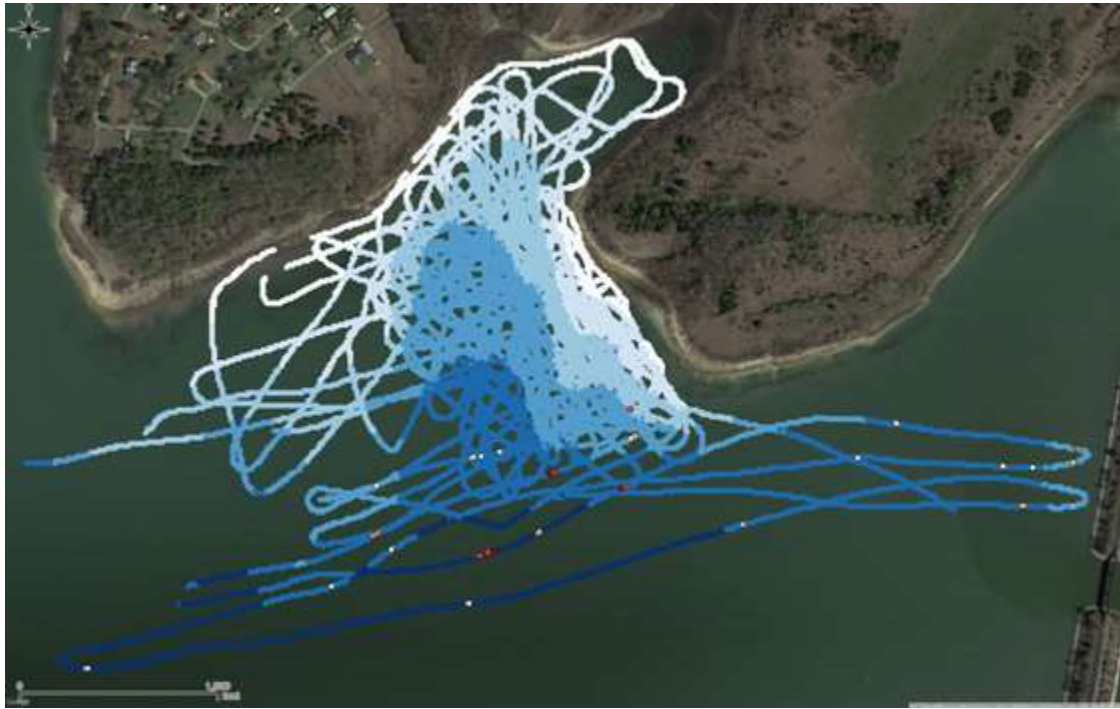


Figure F.2 – Dual Channel Hazards Identified April 15, 2015

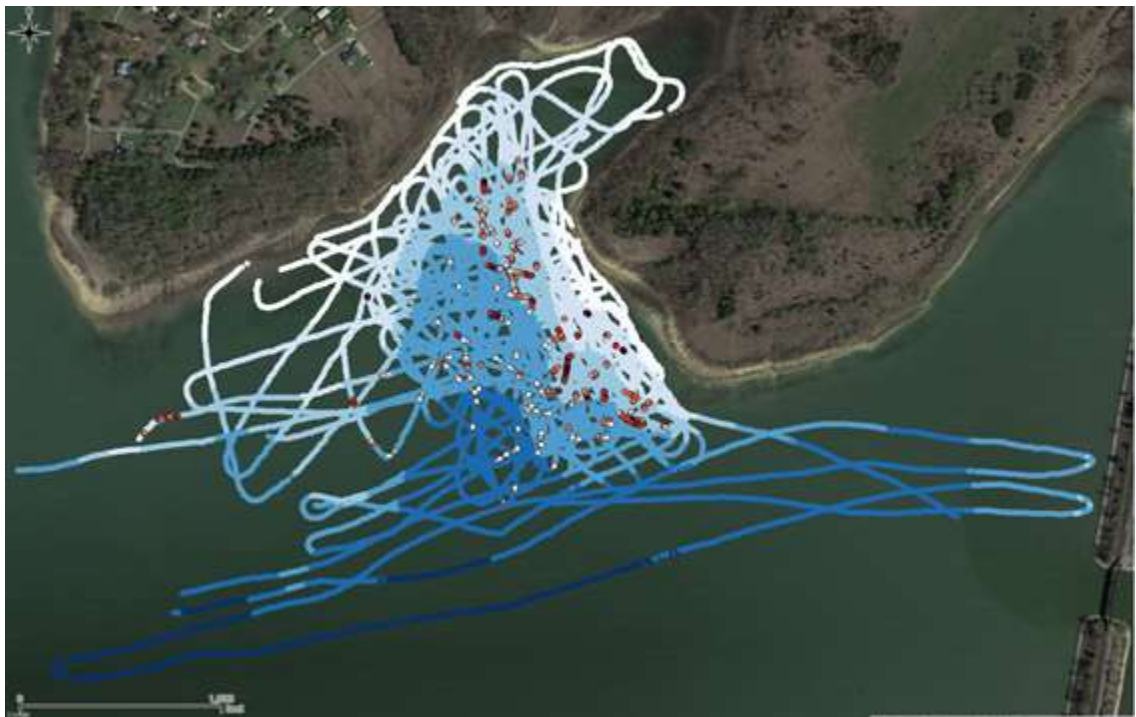


Figure F.3 – Dual Channel Hazards Identified May 1, 2015

REFERENCES

- [1] Stoler, Steve. "With low water levels, Lake Ray Hubbard reveals dangers below." *WFAA*. August 19, 2014. <http://www.wfaa.com/story/news/local/2014/08/19/14091188/>.
- [2] Polsen, Gary, P.E. "Approaches to Prevent Outboard Motors From Flipping Into Boats After Striking Floating or Submerged Objects." December 27, 2014. <http://www.propellersafety.com/wordpress/wp-content/uploads/prevent-outboards-flipping-into-boats.pdf>.
- [3] "BEWARE OF HAZARDS DUE TO LOW LAKE LEVELS." *Brazos River Authority*, July 22, 2009.
- [4] Powell, Steven. "Lake Texoma Officials: lowest lake levels since '70s." *KXII News 12*, January 14, 2014. <http://www.kxii.com/home/headlines/Lake-Texoma-Officials-lowest-levels-since-70s-240192551.html>.
- [5] Cokely, Kevin. "Boaters Urged to Use Caution on North Texas Lakes." *NBC DFW*, May 5, 2014. <http://www.nbcdfw.com/weather/stories/Boaters-Urged-to-Use-Caution-on-North-Texas-Lakes-257723941.html>.
- [6] Lucia, Andrea. "Low Water Levels Causing Major Lake Hazards." *CBS DFW*, September 2, 2013. <http://dfw.cbslocal.com/2013/09/02/low-water-levels-causing-major-lake-hazards/>.
- [7] Lewis, Bob. "Falling Lake Level a Big Problem." *Planet Rockwall*, September 2013. http://planetrockwall.com/news/article/falling_lake_levels_a_big_problem.
- [8] Mashhood, Farzod. "LCRA warns of emerging boating, swimming hazards on Lake Travis." *Statesman*, June 21, 2011. <http://www.statesman.com/news/news/local/lcra-warns-of-emerging-boating-swimming-hazards--1/nRb3c/>.
- [9] Installation and Operations Manual 858c, 898c SI, 958c, 998c S, *Marine Electronics Group of Johnson Outdoors*, 2010.
- [10] Lake Lavon Fishing Forum. <http://forum.lakelavonfishing.com/>.
- [11] Texas Fishing Forum. <http://texasfishingforum.com/>.
- [12] Navionics. <http://www.navionics.com/en>.
- [13] Google Earth. <https://www.google.com/earth/>.

- [14] Blondel, Phillippe. *The Handbook of Sidescan Sonar*. Chichester, Berlin: Springer, 2009.
- [15] Reed, S., Y. Petillot, and J. Bell. "Automated Approach To Classification Of Mine-Like Objects In Sidescan Sonar Using Highlight And Shadow Information." *IEE Proceedings - Radar, Sonar and Navigation* 151, no. 1 (2004): 48-56.
- [16] Chappel, Philip. "Automated Detection and Classification in High-resolution Sonar Imagery for Autonomous Underwater Vehicle Operations." *Maritime Operations Division, DSTO Defence science and Technology Organisation. Commonwealth of Australia*: (December 2008).
- [17] Goillet, J.R., J.K. Sailor, J.K Berry, and K. Sherman. "Computer-Assisted Map Analysis of Marine Ecosystem Information." *OCEANS* (September 1981): 264-272
- [18] Grafarend, Erik W, and Friedrich W Krumm. *Map Projections*. Berlin: Springer, 2006.
- [19] Snyder, John P. "Map Projections - A Working Manual." U.S. Geological Survey Professional Paper 1395. *United States Government Printing Office*. Washington, D.C: (1987).
- [20] Bager, John W., Larry L. Fry, Sandra S. Jacks, and David R. Hill. "Technical Manual 8358.1 Datums, Ellipsoids, Grids, and Grid Reference Systems." The Defence Mapping Agency. February 23, 1996.
- [21] Moravec, H.P. and A. Elfes. "High resolution maps from wide angle sonar." *1985 IEEE International Conference on Robotics and Automation. Proceedings 2* (March 1985): 116-121.
- [22] Elfes, A. and L. Matthies. "Integration of sonar and stereo range data using a grid-based representation." *IEEE International Conference on Robotics and Automation 2* (April 1988): 727-733
- [23] Berger, J.O. *Statistical Decision Theory and Bayesian Analysis*. Berlin: Springer-Verlag. 1985.
- [24] Wallner, F., and R. Dillman. "Real-Time Map Refinement By Use Of Sonar And Active Stereo-Vision." *Robotics and Autonomous Systems* 16, no. 1 (1995): 47-56.

- [25] Konolidge, K. "Improved Occupancy Grids for Map Building." *Autonomous Robots* 4 (1997): 351–367.
- [26] Payeur, P., P. Hebert, D. Laurendeau, and C. M. Gosselin. "Probabilistic octree modeling of a 3D dynamic environment." *IEEE International Conference on Robotics and Automation, Proceedings 2* (April 1997): 1289–1296.
- [27] Gindele, T., S. Brechtel, J. Schroder, and R. Dillmann. "Bayesian Occupancy grid Filter for dynamic environments using prior map knowledge." *IEEE Intelligent Vehicles Symposium* (June 2009): 669–676.
- [28] Jessup, James, Sidney N. Givigi, and Alain Beaulieu. "Robust And Efficient Multirobot 3-D Mapping Merging With Octree-Based Occupancy Grids." *IEEE Systems Journal* (2015): 1-10.
- [29] Calder, B.R., L.M. Linnett, and D.R. Carmichael. "A Bayesian approach to object detection in sidescan sonar." *Sixth International Conference on Image Processing and Its Applications 2* (July 1997): 857–861.
- [30] Carmichael, D., "Image processing techniques for the analysis of sidescan sonar survey data," *IEE Colloquium on Underwater Applications of Image Processing* 217 (March 1998): 31-36
- [31] Kaeser, Adam J., and Thomas L. Litts. "A Novel Technique For Mapping Habitat In Navigable Streams Using Low-Cost Side Scan Sonar." *Fisheries* 35, no. 4 (2010): 163-174.
- [32] Kaeser, Adam J., Thomas L. Litts, and T. Wesley Tracy. "USING LOW-COST SIDE-SCAN SONAR FOR BENTHIC MAPPING THROUGHOUT THE LOWER FLINT RIVER, GEORGIA, USA". *River Res. Applic.* 29, no. 5 (2012): 634-644.
- [33] Kaeser, Adam J., and Thomas L. Litts. "An Illustrated Guide to Low-cost, Side Scan Sonar Habitat Mapping". Georgia Department of Natural Resources, April 2013.
- [34] Guo, J., W.H. Wang, S.W. Huang, E. Chen, and F.C. Chiu. "Map uncertainties for unmanned underwater vehicle navigation using sidescan sonar." *OCEANS 2010 IEEE - Sydney* (May 2010): 1 – 10.
- [35] OpenCV. <http://opencv.org/>.
- [36] Tesseract OCR. <http://code.google.com/p/tesseract-ocr/>.
- [37] Humminbird Side Imaging Forums. <http://forums.sideimagingsoft.com>.

- [38] QGIS. <http://www.qgis.org/>.
- [39] “Lavon Lake”, *United States Army Corps of Engineers, Fort Worth District*.
<http://www.swf-wc.usace.army.mil/lavon/Information/index.asp>.
- [40] HumViewer. <http://humviewer.cm-johansen.dk/>.
- [41] Rango, A., A. Laliberte, K. Havstad, C. Winters, C. Steele, and D. Browning. "Rangeland resource assessment, monitoring, and management using Unmanned Aerial Vehicle-based remote sensing." *IEEE International Geoscience and Remote Sensing Symposium (IGARSS)* (July 2010): 25-30.
- [42] Manley, J.E. "Unmanned surface vehicles, 15 years of development." *OCEANS 2008* (September 2008): 1 – 4.
- [43] Heidarsson, H.K. and G. Sukhatme. "Obstacle detection and avoidance for an Autonomous Surface Vehicle using a profiling sonar." *2011 IEEE International Conference on Robotics and Automation (ICRA)* (May 2011): 731-736.
- [44] Quidu, I., J.P. Malkasse, G. Burel, and P. Vilbe. "Mine classification using a hybrid setof descriptors." *OCEANS 2000 MTS/IEEE Conference and Exhibition 1* (2000): 291-297.
- [45] Guillaudeux, S., S. Daniel, and E. Maillard. "Optimization of a sonar image processing chain: a fuzzy rules based expert system approach." *OCEANS '96. MTS/IEEE. Prospects for the 21st Century. Conference Proceedings 3* (September 1996): 1319-1323.
- [46] Mignotte, M., C. Collet, P. Perez, and P. Bouthemy. “Sonar Image Segmentation Using An Unsupervised Hierarchical MRF Model.” *IEEE Trans. on Image Process.* 9, no. 7 (2000): 1216-1231.
- [47] Reed, Scott, Yvan Petillot, and Judith Bell. “Model-Based Approach To The Detection And Classification Of Mines In Sidescan Sonar.” *Applied Optics* 43, no. 2 (2004): 237-246.
- [48] Solis, Rubin S., P.E. “Volumetric and Sedimentation Survey Lavon Lake June – July 2011 Survey.” *Texas Water Development Board*, January 2013.
- [49] NOAA, National Oceanic and Atmospheric Administration, United States Department of Commerce. <http://oceanexplorer.noaa.gov/technology/tools/sonar/sonar.html>.

[50] Woods Hole Coastal and Marine Science Center, United States Geological Survey.
http://woodshole.er.usgs.gov/operations/sfmapping/sonar_xtf.htm

[51] Young, Micheal E. “Deep and wide: Lake lovers urged to beware of high-water Hazards.” *Dallas Morning News*, May 19, 2015. <http://www.dallasnews.com/news/metro/20150519-deep-and-wide-lake-lovers-urged-to-beware-of-high-water-hazards.ece>.

[52] Microsoft Bing Maps. <https://www.bing.com/maps/>.

